J. theor. Biol. (1998) **193,** 131–151
Article No. jt980692

Chlorophyll *a* Fluorescence Induction in Higher Plants: Modelling and Numerical Simulation

ALEXANDRINA STIRBET,*† GOVINDJEE,‡ BRUNO J. STRASSER* AND RETO J. STRASSER*

**Bioenergetics Laboratory*, *University of Geneva*, *CH*-1254 *Lullier-Jussy/Geneva*, *Switzerland*
†Department of Biophysics, *University of Bucharest*, *R*-76900 *Bucharest*, *Romania*

(*Received on* 22 *December* 1997, *Accepted on* 17 *February* 1998)

Chlorophyll *a* fluorescence induction is extensively used as a probe of photosynthesis, and thus, it has become necessary to quantitatively analyse it to extend its usefulness. We simulate the experimental data of fluorescence transients in strong light through numerical integration, both in dark- and light-adapted plants. In the mathematical model used here we have considered for the first time the redox reactions at both the acceptor and the donor sides of photosystem II, and the non-photochemical quenching by the oxidised plastoquinone molecules from the lipid matrix of the thylakoid membrane. The model is based on assumptions established in the literature and also the values of input parameters used in simulations. The simulated fluorescence induction curves show the characteristic O → J → I → P steps as in the experimental ones and, in specific conditions, the presence of a dip (D) between the I and P steps of the transient. Moreover, it has been shown here how typical patterns of fluorescence kinetics are influenced by the state of the sample by studying the basic effects of the influence of some parameters [i.e. the connectivity between different PS II units, initial Q_B:Q_B^- ratio and the ratio of the starting states of the oxygen evolving complex (S_1:S_2), number of plastoquinone molecules in the plastoquinone pool, initial redox state of the plastoquinone pool, and the rate of plastoquinol oxidation]. In this way the information can be drawn from the experimental curves relative to these parameters.

© 1998 Academic Press

Introduction

Chlorophyll *a* (Chl *a*) fluorescence induction observed in plants, algae and cyanobacteria, known also as the fluorescence transient or Kautsky effect (Kautsky & Hirsch, 1931), has been extensively studied (see reviews, Govindjee & Papageorgiou, 1971; Papageorgiou, 1975; Fork & Mohanty, 1986; Krause & Weis, 1991; Dau, 1994; Joshi & Mohanty, 1995; Govindjee, 1995). It consists of light intensity dependent polyphasic changes in Chl *a* fluorescence emission when a dark-adapted leaf, or a suspension of isolated chloroplasts or intact photosynthetic cells, is illuminated with continuous light (see Fig. 1, curves 1 and 2). In the first phase of the transient (time-scale from zero to one or several seconds, depending on the light intensity) the fluorescence intensity rises quickly from an initial low value, F_0 (the O level), to a higher one, F_P (the P level). Under low light, fluorescence rises to an intermediary step denoted as F_{pl} (curve 1, Fig. 1), but under high light, typically over 500 W m^{-2}, two intermediary steps designated as F_J (the "J" or the I_1 level) and F_I (the "I" or the I_2 level) normally appear (curve 2, Fig. 1; see Strasser & Govindjee, 1991, 1992; Neubauer & Schreiber, 1987). The F_P level becomes saturated from 100 Wm^{-2} and is then denoted as F_M. A dip between I and P is sometimes present in fluorescence transients and is labelled as D (Munday & Govindjee, 1969).

It is well established now that the variable fluorescence $F_V(t)$ [defined as $F(t) - F_0$, where $F(t)$ is the fluorescence intensity at any time t] is related

‡ On sabbatical from Department of Plant Biology, University of Illinois, 265 Morril Hall, Urbana, IL 61801, U.S.A.

0022–5193/98/130131 + 21 $30.00/0
© 1998 Academic Press

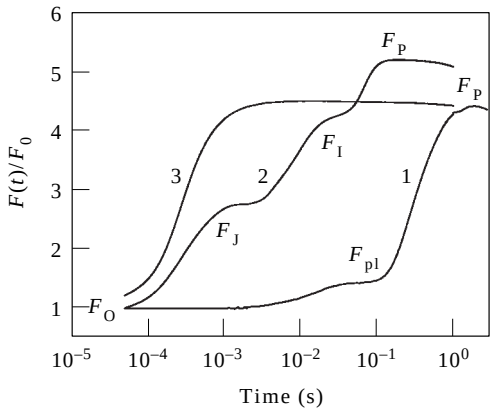

FIG. 1. Fast Chl *a* fluorescence induction curves (fluorescence as a function of time—from 50 μs to 1 s) measured on dark adapted *Pisum sativum* leaves illuminated with 12 Wm^{-2} (curve 1), 600 Wm^{-2} (curve 2), and 600 Wm^{-2} in the presence of DCMU (curve 3). Wavelength of illumination, 650 nm. For definition of symbols, see Glossary.

mainly to the fluorescence of the antenna chlorophyll of photosystem II (PS II), and is due to the variation of the quantum yield of fluorescence emission (between 2 and 10%) (Latimer *et al*., 1956). The interpretation of the fluorescence signals must always take into account that the quantum yield of Chl *a* fluorescence is proportional to the rate constant of fluorescence divided by the rate constants of all the various pathways of deexcitation (i.e. fluorescence, heat dissipation, excitation energy transfer, quenching, and photochemistry).

As the fluorescence induction measurements are now frequently used in different *in vivo* studies of plants, such as stress, pollution and productivity (see e.g. Schreiber & Bilger, 1993), it is very important to know how to correlate the experimental results with the rates of specific biochemical reactions. Therefore, a mathematical model that can be used to simulate and fit the measured data is considered to be very useful. However, most earlier simulations have been made for the simpler case of chloroplasts inhibited with diuron (DCMU) (Hsu *et al*., 1989; Trissl *et al*., 1993; Trissl & Lavergne, 1994; and Lavergne & Trissl, 1995), where the fluorescence transient has only an O–J (or O–P shape) (curve 3, Fig. 1), or for chloroplasts illuminated with low light intensities (curve 1, Fig. 1) (Renger & Schulze, 1985; Baake & Strasser, 1990; Baake & Schlöder, 1992; Hsu, 1992, 1993).

In this paper, we present a model that simulates experimental O–J–I–(D)–P fluorescence curves obtained upon exposure of dark-adapted photosynthetic apparatus with continuous strong light illumination (curve 2, Fig. 1). Preliminary observations have been presented (see Stirbet & Strasser, 1995, Stirbet *et al*., 1995, and Stirbet & Strasser, 1996). The model is based on six main assumptions: (1) Chl *a* fluorescence reflects the concentration of the reduced electron acceptor Q_A (Duysens & Sweers, 1963); (2) for all practical purposes, the PS II units are considered homogeneous; (3) excitation energy can be exchanged between several PS II units (Joliot & Joliot, 1964); (4) the rate constant of the Q_A reduction is modulated by the redox state of the oxygen evolving complex (OEC), the so-called S-states (Delosme, 1971 ; Joliot *et al*., 1971); (5) oxidised plastoquinone pool molecules quench Chl *a* fluorescence (Vernotte *et al*., 1979); and (6) a so-called "two-electron-gate process" acts on the acceptor side of PS II (Velthuys & Amesz, 1974; Bouges-Bocquet, 1973). In order to prove the generality of the model, we have also simulated specific fluorescence curves such as those obtained with DCMU treatment or with pre-illumination (light-adaptation) of the leaf.

Modelling of the Fast Phase of Chl *a* Fluorescence Induction: Theory and Assumptions

Chl *a* fluorescence emission *in vivo* comes from both PS I and PS II photosystems, the contribution of PS I being smaller (10–25% of F_0—see Lavergne & Trissl, 1995). As PS I does not contribute to the variable fluorescence (Butler, 1978), it was not considered here. However, the use of uncorrected fluorescence transients (neglecting PS I contribution) causes the values of the ratio $N = F_V/F_0$ and of the connectivity parameter C (see below) to be slightly under-evaluated. In this paper we only simulate the variable fluorescence induction curves and do not fit them exactly with the experimental data; so neglecting the contribution of PS I fluorescence does not affect the results.

The first phase of Chl *a* fluorescence induction is mainly related to the photochemical processes and charge separation reactions that take place at the PS II level (Dau, 1994; Govindjee, 1995; Joshi & Mohanty, 1995). Therefore, for the modelling of the fluorescence transients to be precise, the structure and function of these reaction centres must be defined.

The PS II unit catalyses the light-induced electron transport from water to the plastoquinone (PQ) pool molecules (mobile electron carriers between PS II and PS I). Figure 2 shows a schematic view of the main electron transport mediated by PS II, in which, besides water and PQ pool molecules, six other components are involved: (1) the water-oxidising manganese cluster (denoted also as Oxygen Evolving Complex, OEC); (2) the redox-active tyrosine, Y_Z;

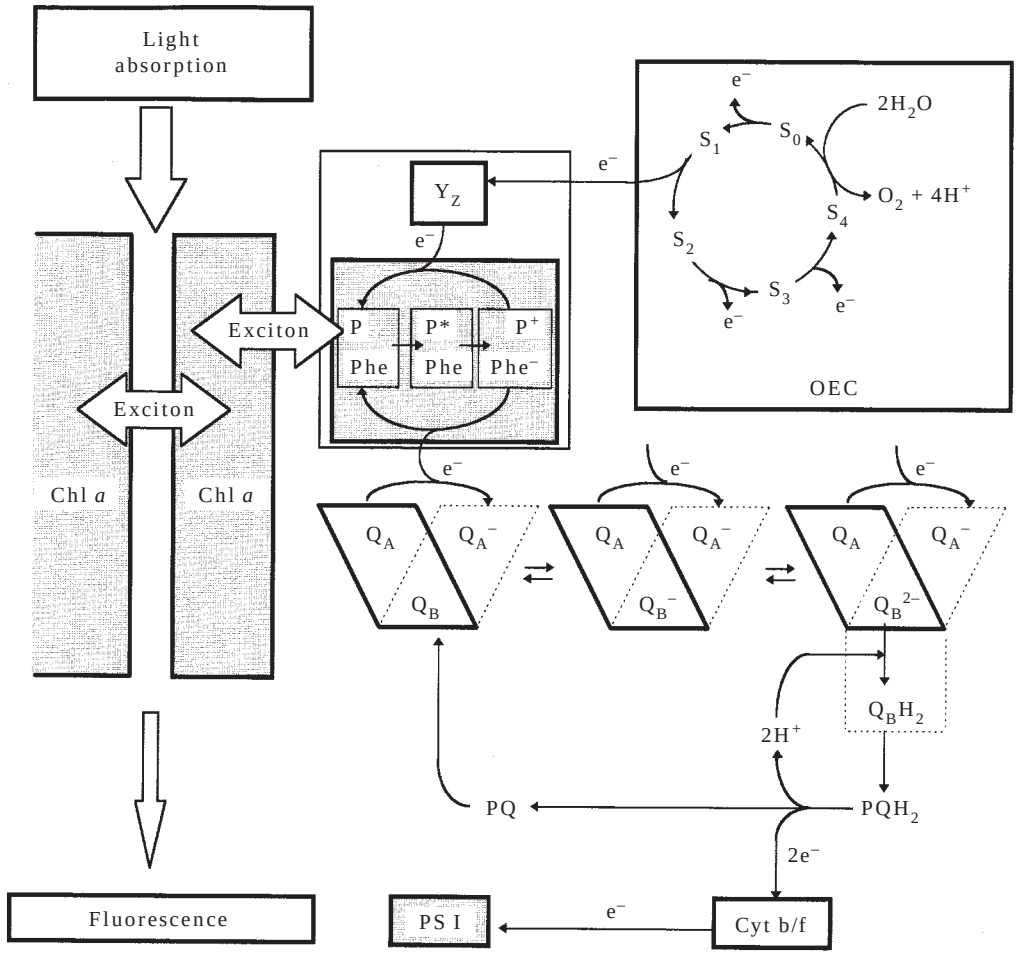

FIG. 2. A schematic diagram of electron transport reactions considered in the model (see text for explanation). Chl *a* = chlorophyll *a* antenna; OEC = oxygen evolving complex in S_n states; Y_Z = primary electron donor to $P680^+$; P = P680, the PS II reaction centre Chl *a*; Phe = pheophytin *a*; Q_A, Q_B = bound plastoquinones; PQ = plastoquinone pool; Cyt b/f = cytochrome b_6/f complex; PS I = photosystem I.

(3) the photochemical reaction centre (P680) which is the primary electron donor of PS II; (4) one pheophytin *a* molecule (Phe) which is the primary electron acceptor of PS II; (5) one tightly bound plastoquinone (Q_A); and (6) one loosely bound plastoquinone (Q_B). Kinetic measurements support this theory of the structure of the main electron transport chain (see reviews by Hansson & Wydrzynski, 1990; Seibert, 1993; Diner & Babcock, 1996, 1977). There are evidences for some side pathways of electron transport, but these are ignored in the present model.

The electron transport at PS II level starts with the exciton trapping by the photochemical reaction centre chlorophyll *a* (P680) which induces the primary charge separation: $P680^+Phe^-$ (Greenfield & Wasielewski, 1996). This primary radical pair can decay by several pathways: transfer of the electron from Phe^- to Q_A (the secondary charge separation), recombination and reformation of singlet excited state of the photochemical reaction centre P680*, formation of P680 triplet state, and other non-radiative pathways. Under normal conditions, electron flow from Phe^- to Q_A is the major reaction. Q_A, which is a one-electron acceptor, stabilises the charge separation. Subsequently, the reduction of $P680^+$ to P680 occurs by the transfer of one electron from Y_Z. Q_A^- reduces a plastoquinone molecule, Q_B, loosely bound to a specific site on PS II centre, named the Q_B-binding site (Crofts & Wraight, 1983). The full

reduction of Q_B requires the addition of two electrons; therefore, two photochemical turnovers of the reaction centre are needed (two-electron gating mechanism). Velthuys (1981) has suggested that Q_B^- remains bound at the Q_B-binding site before the second reduction, as the affinity of Q_B binding site is low for PQ and PQH_2, but high for Q_B^-. Only after the protonation of Q_B^{2-} does the plastoquinol ($Q_BH_2 = PQH_2$) unbind from the reaction centre and diffuse into the membrane. Then, an oxidised plastoquinone molecule will (eventually) bind to the Q_B-binding site, and the process of Q_B reduction can be repeated.

On the donor side of PS II unit, the oxidised Y_Z is reduced by OEC. The rate constant for this process depends on the redox state of the water-oxidising manganese cluster (Babcock *et al*., 1976). It has been proposed that this dependence is due to electrostatic effects. The OEC cycles through the so-called S_n states (see Fig. 2), the subscript indicating the number of oxidising equivalents in the system. The stepwise accumulation of four positive charges on the oxidising side of PS II constitutes a condition for the splitting of two water molecules and the release of four electrons, four protons and of molecular oxygen (Kok *et al*., 1970). The oxygen molecule is released during the S_4 to S_0 transition (for reviews, see Renger, 1993; Britt, 1996).

The electron transport chain described above, dealing with the redox reactions around the PS II centre, is schematically illustrated in Fig. 2. We have used this reaction scheme in the kinetic analysis of the photosynthetic system. Similar to the models of Renger & Schulze (1985) and Hsu (1992), the exciton trapping ($P680 \rightarrow P680^*$) and the primary charge separation ($P680^*Phe \rightarrow P680^+Phe^-$) have been introduced indirectly in the model through the rate constant of Q_A reduction, kL. This one is a global rate constant and depends on several parameters, for example light intensity, absorption cross section of the antenna of PS II units, rate constants of exciton trapping and primary charge separation. The reverse reaction represents the complex process of charge recombination.

In the photosynthetic membranes, the PS II centres do not function in an isolated state. An efficient excitation energy transfer between several PS II units takes place, that increases the efficiency of the light conversion process. This process is commonly denoted as PS II connectivity (Joliot & Joliot, 1964; Joliot *et al*., 1973) or grouping (Strasser, 1978 and 1981).

It is well known that during the exposure to light of a dark adapted green plant, the primary quinone acceptor Q_A accumulates in its reduced form Q_A^- (see for example the review on Chl *a* fluorescence induction phenomenon by Govindjee, 1995). The net Q_A^- accumulates as the plastoquinone molecules of the PQ pool become reduced. The plastoquinol (PQH_2) is reoxidised by the cytochrome b_6/f complex (Cyt b/f), this being the limiting reaction of the linear electron transport chain (Stiehl & Witt, 1969; Haehnel, 1984). Since the oxidised Q_A is a strong quencher of the PS II fluorescence (Duysens & Sweers, 1963), the accumulation of the reduced Q_A seems to be the main factor that must be considered when the fluorescence induction is analysed. The photochemical reaction centre of PS II in its oxidised state, $P680^+$, is also an efficient fluorescence quencher (Butler, 1972; Sonneveld *et al*., 1979; Deprez *et al*., 1983; Shinkarev & Govindjee, 1993). However, we will not consider $P680^+$ quenching here, because under most conditions, there is no significant accumulation of $P680^+$ as the abundant water molecules keep it reduced via OEC and the primary donor Y_Z (Dau, 1994).

ASSUMPTIONS OF THE MODEL

In view of the above, since the concentrations of Q_A^- and $P680^+$ depend mainly on the processes occurring at the PS II level, *the first assumption* of our model of the fast phase of Chl *a* fluorescence induction is that the variable fluorescence is related mainly to PS II kinetics. More specifically, Chl *a* fluorescence yield mainly reflects the number of the closed PS II centres during the time interval of our analysis. However, PS I activity is also indirectly considered, as the rate constant of plastoquinol reoxidation by the Cyt b/f complex depends on the rate of reduction of the PS I photochemical reaction centre in its oxidised state ($P700^+$). It must be noted that, for simplicity, in the present model we have considered the reoxidation reaction of plastoquinol to have a first order kinetics.

The second assumption of the model is that, on average, all PS II units have the same kinetic characteristics (a homogeneous PS II population), and each one of them is served by the same number of PQ pool molecules.

The third assumption of the model is that the fraction of closed reaction centres, $B(t) = [Q_A^-]_{total}(t)/([Q_A^-]_{total}(t) + [Q_A]_{total}(t))$, influences the relative variable fluorescence, $V(t) = [F(t) - F_0]/(F_M - F_0)$, and the "global" reduction rate of Q_A, kL. Furthermore, according to the theory of the PS II connectivity (Joliot & Joliot, 1964; Strasser, 1978; Butler, 1980; Strasser, 1981; Trissl & Lavergne, 1994; and Lavergne & Trissl, 1995) the following relationships are valid:

$$V(t) = \frac{B(t)}{1 + C[1 - B(t)]}; \qquad (1)$$

$$kL = kL^0 \frac{1 + C}{1 + C[1 - B(t)]}; \quad (2)$$

where C will be referred as the connectivity parameter (its value depending on the overall probability of connectivity between the PS II units—see Joliot & Joliot, 1964; Strasser, 1978; and Butler, 1980) and kL^0 is the initial rate constant of Q_A reduction. It can be seen that if the photosystems are not connected (i.e. $C = 0$) the relative variable fluorescence is identical to the fraction of closed reaction centres, $V(t) = B(t)$, and the rate constant of Q_A reduction is constant, $kL = kL^0$.

The fourth assumption of our model is that the net rate of Q_A reduction (kL) depends also on the S_n state of OEC, it being higher in S_0 and S_1 than in S_2 and S_3 states. This assumption is based on the observation of Delosme (1971) and Joliot *et al*. (1971), that open PS II units in the S_0 and S_1 states are better quenchers of fluorescence than in the S_2 and S_3 states. There are two possibilities: increased rate of photochemistry and/or of heat dissipation. We favour the first; therefore, this different quenching capacity is assumed to be due to a higher primary rate constant for photochemistry (kL) for PS II units in the S_0 and S_1 state. The following relationship between the initial rate constants of Q_A reduction, kL^0, have been used in the simulations:

$$kL_0^0 = kL_1^0 = 2kL_2^0 = 2kL_3^0 \quad (3)$$

where the subscripts refer to the redox state of OEC in PS II unit (i.e. S_0, S_1, S_2, and S_3, respectively).

The fifth assumption of the model is that Chl *a* fluorescence in leaves is quenched also by the oxidised molecules of the PQ pool (Vernotte *et al*., 1979). These authors have shown that the quenching is of Stern–Volmer type, similar to that obtained with exogenous quinones (e.g. dimethylbenzoquinone and dichlorobenzoquinone—see Lavergne & Leci, 1993; and Srivastava *et al*., 1995a). It is interesting to note that for both endogenous and exogenous quinones, the Stern-Volmer constant was found approximately four times higher for F_M than for F_0 (Vernotte *et al*., 1979; Srivastava *et al*., 1995a).

Therefore, the values of the relative variable fluorescence, $V(t)$, have been calculated from the unquenched ones, $V^u(t)$, by using the Stern–Volmer relationship. Because several restrictive assumptions have been used in the estimation of the impact of the PQ non-photochemical quenching effect on the relative variable fluorescence, the obtained semi-empirical relationship (A.7) is only an approximation (see Appendix). The experimental data used in this formula were f^{cl} and f^{op} (the fractions of fluorescence intensity reduced by PQ non-photochemical quenching for a system with all PS II units closed and open, respectively) and the ratio $N = F_V/F_0 = (F_M - F_0)/F_0$. We have used the values $f^{cl} = 0.3$, $f^{op} = 0.1$ (Vernotte *et al*., 1979), and $N = 4$ (Srivastava *et al*., 1995b).

Materials and Methods

EXPERIMENTAL MEASUREMENTS

In this paper, we have compared our theoretical curves with the data of Strasser *et al*. (1995) on fluorescence transients of dark-adapted and light-adapted leaves. Since these measurements are important to this paper, we have repeated them, and describe below the experimental conditions of these measurements that confirm the earlier observations of Strasser *et al*. (1995).

Plant material

Experiments were done with fully mature intact leaves of 3–4 week old pea (*Pisum sativum*). Plants were grown in the greenhouse in small pots with a soil mixture Optima (Optima-Werke H. Gilgen, Munchenstein, Switzerland), at 22°C/18°C (day/night) temperature cycle under natural sunlight, with alternate day watering.

Chl a *fluorescence induction measurements*

Chl *a* fluorescence transients from pea leaves were measured at room temperature, using a shutter-less system (Plant Efficiency Analyser built by Hansatech Ltd., King's Lynn, Norfolk, U.K.). Light was provided by an array of six light-emitting diodes (peak at 650 nm) focused on the sample surface to provide homogeneous illumination over the exposed area of the sample (4 mm diameter). The light intensity was 600 Wm^{-2}, for high light conditions, and 12 Wm^{-2}, for low light conditions. The fluorescence signals were detected using a PIN-photodiode after passing through a long-pass filter (50% transmission at 720 nm). The first reliable point of the transient is measured 50 μs after the onset of illumination. This point was taken as F_0 as extrapolation of fluorescence to time zero was within 5% of this value.

Fluorescence measurements were taken in dark adapted conditions (leaves maintained 20 min in darkness), or in light adapted conditions (leaves illuminated continuously for 1 hr with 180 Wm^{-2} light intensity and then dark adapted for 30 s).

NUMERICAL SIMULATION PROCEDURE

The concentration of reactants in a 0.5 s time range have been obtained through numerical integration of Ordinary Differential Equations systems (ODEs) associated with the reactions presented in Fig. 3(a) and (b). In these figures the reaction chains related to PS II units which are initially in $S_1Q_AQ_B$ and $S_0Q_AQ_B^-$ states [Fig. 3(a)], and in $S_0Q_AQ_B$ and $S_1Q_AQ_B^-$ states [Fig. 3(b)] are shown. For simplicity, we have normalised the total number of PS II centres in different redox states and the total number of plastoquinones in the pool. For example, at time zero:

$$[S_1Q_AQ_B] + [S_0Q_AQ_B^-] + [S_0Q_AQ_B] + [S_1Q_AQ_B^-] = 1$$

and

$$[PQ] + [PQH_2] = n$$

where n is the total number of the plastoquinone molecules in the pool.

The PS II units with Y_Z and P680 in the oxidised states (Y_Z^+ and/or $P680^+$) have been noted with an asterisk after S_n (e.g. $S_3{*}Q_A^-Q_B$). Those $S_n \rightarrow S_{n+1}$ transitions that are much faster than the following (succeeding) reaction in the chain (e.g. $S_0 \rightarrow S_1$ transition compared to $Q_A^-Q_B \rightarrow Q_AQ_B^-$ reaction—see Table 1 for the corresponding rate constants) have been considered to take place simultaneously with the light reaction, in order to reduce the number of equations in the ODE systems. All the reactions in the considered model are of first order (except Q_BH_2-PQ exchange reaction, which is of second order) and with a kinetics of mass action type. The loosely bound plastoquinol molecule (Q_BH_2) is replaced by a new PQ molecule from the pool, and it diffuses to the oxidation site on the Cyt b/f complex. We have considered that the Q_B-site is always occupied (with Q_B, Q_B^-, Q_B^{2-}, or Q_BH_2). Also, at the beginning of illumination we have assumed that all of the PS II units are in the open state (i.e. the fraction of closed reaction centres equal to zero, $B = 0$) for both types of samples, the dark adapted and the light adapted leaves.

The numerical algorithm used for the simulations was the Livermore Solver of Ordinary Differential Equations (LSODE) procedure (Hindmarsch, 1980), with the initial concentrations of the reactants and the rate constants of the reactions as parameters. We have used the values of the rate constants presented in Table 1 (unless otherwise noted). These values are comparable to those reported in the literature (see references in Table 1).

Before simulating the experimental O–J–I–P curves, it was necessary to evaluate the rate constant for Q_A reduction of the reaction centres in state S_1 (kL_1^0) in our specific experimental conditions (600 Wm^{-2} illumination intensity, pea leaves). It was obtained by comparing the simulated transients for different values of kL_1^0, and the experimental one of DCMU treated leaves. Theoretical curves have been

TABLE 1

The values of input parameters used in simulations and the corresponding values from literature

Input parameters	Dark adapted leaf	Light adapted leaf	Reported values	References
$N = F_V/F_0$	4	2	2–4	Srivastava *et al.* (1995b)
f^{cl}; f^{op}	30%; 10%	30%; 10%	30–20%; 5–10%	Vernotte *et al.* (1979)
Total number of PQ in the pool; (initial ratio $PQ:PQH_2$)	6; (6:0)	6; (4:2)	5–10	Lavergne *et al.* (1992)
Initial ratio: $S_1:S_0$	0.8:0.2	0.8:0.2	0.75:025	Kok *et al.* (1970) Forbush *et al.* (1971)
Initial ratio: $Q_B:Q_B^-$	0.7:0.3	0.7:0.3	0.7:0.3 0.5:0.5	Wollman (1978) Rutherford *et al.* (1984)
$t_{1/2}$; and K_{eq} for: $Q_A^-Q_B \leftrightarrow Q_AQ_B^-$	230 μ; 20	230 μs; 20	100–200 μs; 15–20	Diner, 1977 Robinson & Crofts (1983)
$t_{1/2}$; and K_{eq} for: $Q_A^-Q_B^- \leftrightarrow Q_AQ_B^{2-}$	460 μs; 10	460 μs; 1	300–500 μs; 50 or 1	Diner (1977) Crofts & Wraight (1983)
${}^2t_{1/2}$; and K_{eq} for: $Q_AQ_BH_2 + PQ \leftrightarrow Q_AQ_B + PQH_2$	1 ms; 10	1 ms; 10	1 ms; 1 or 10	Crofts *et al.* (1984)
$t_{1/2}$ for: $PQH_2 \rightarrow PQ$	10 ms	3.5 ms	4–10 ms	Haehnel (1976)
$t_{1/2}$ for: $S_0 \rightarrow S_1$	30 μs	30 μs	30 μs	Babcock (1987)
$t_{1/2}$ for: $S_1 \rightarrow S_2$	110 μs	110 μs	110 μs	Babcock (1987)
$t_{1/2}$ for: $S_2 \rightarrow S_3$	350 μs	350 μs	350 μs	Babcock (1987)
$t_{1/2}$ for: $S_3 \Rightarrow S_4 \rightarrow S_0$	1.3 ms	1 ms	1–1.3 ms	Babcock (1987)

f^{cl} and f^{op} are the fractions of the Chl a fluorescence that have been quenched by the oxidised PQ molecules from the pool, for a system with all PS II units closed and open respectively; $t_{1/2}$ is the half time of a forward first order reaction; ${}^2t_{1/2}$ is the half time of a second order reaction (i.e. the PQ exchange reaction), with ${}^2t_{1/2} = \ln 2/({}^2k_E[PQ]_0)$; and K_{eq} is the equilibrium constant of reaction.

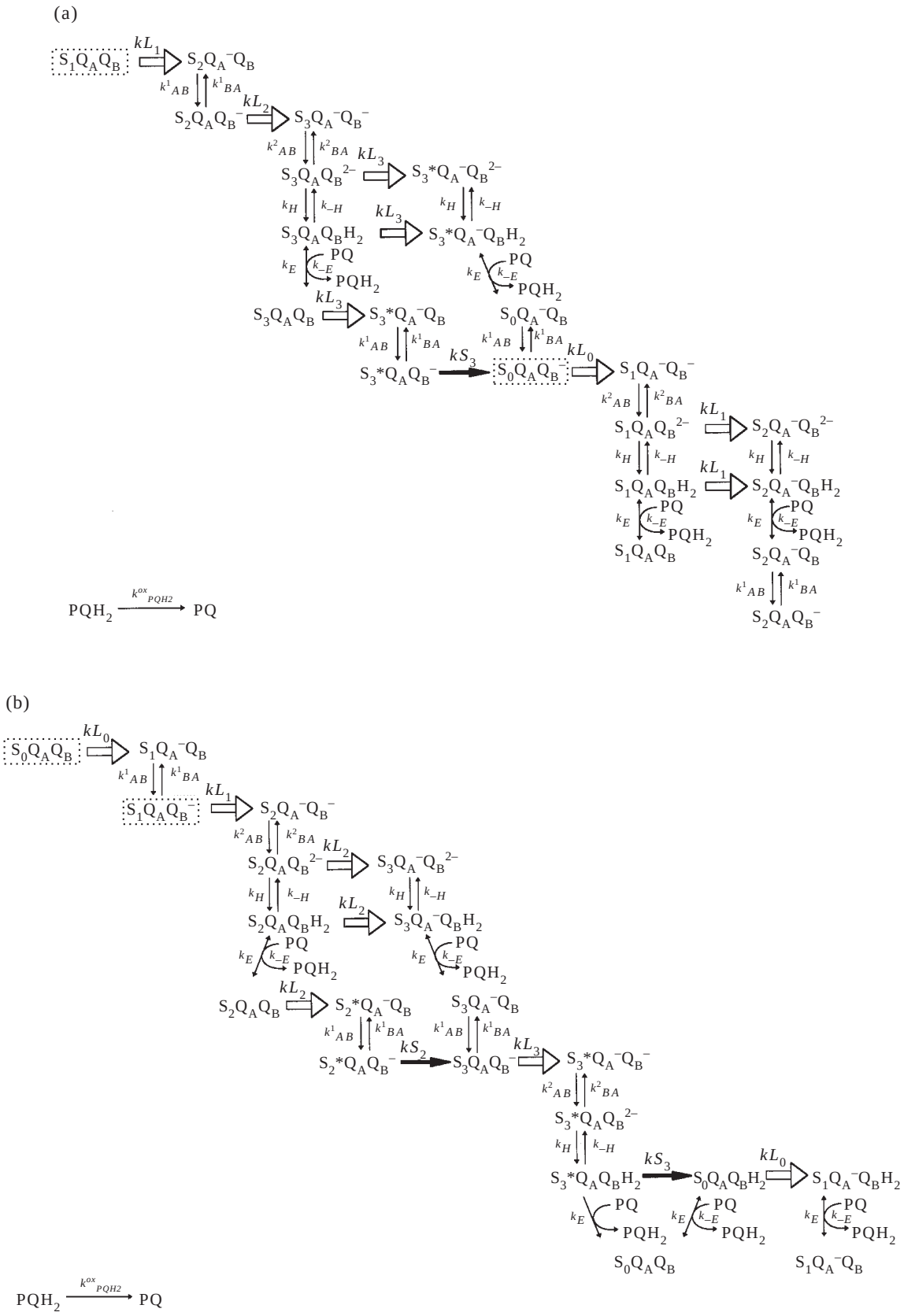

FIG. 3. PS II redox reaction chain for the units initially in (a) $S_1Q_AQ_B$ and $S_0Q_AQ_B^-$ states; (b) $S_0Q_AQ_B$ and $S_1Q_AQ_B^-$ states.

obtained considering the values of the rate constants for Q_B and Q_B^- reduction equal to zero. Similar to the experimental DCMU transient (curve 3, Fig. 1), they have a characteristic O–P shape (or O–J shape, as we may define it) reaching the maximum values ($V = 1$) in several ms (results not shown). The best fit with experimental data was obtained with $kL_1^0 = 2000\ s^{-1}$, and was used in all the simulations presented in this paper (unless otherwise noted).

Finally, the time courses of the various redox states of PS II units ($Q_A^-Q_B$, $Q_A^-Q_B^-$, $Q_A^-Q_B^{2-}$, $Q_A^-Q_BH_2$, Q_AQ_B, $Q_AQ_B^-$, $Q_AQ_B^{2-}$, and $Q_AQ_BH_2$) have been calculated. We have also calculated using eqns (1) and (A.7) (see earlier in the theory and assumptions of the model, and the Appendix, respectively), the time courses of the fraction of reaction centres in which Q_A is reduced (the so-called closed reaction centres), $B(t)$, and the relative variable fluorescence with and without PQ quenching, $V(t)$ and $V^u(t)$, respectively. In order to compare the shapes of the theoretical curves, the ratios $B(t)/B_{max}$, $V(t)/V_{max}$, and $V^u(t)/V^u_{max}$ have been presented (where B_{max}, V_{max} and V^u_{max} are the highest values of $B(t)$, $V(t)$ and $V^u(t)$, respectively).

Results and Discussions

GENERAL REMARKS

The curves obtained from simulations of the transients of dark adapted leaves are presented in Fig. 4(a) and (b). Time courses of the concentrations of closed PS II units (i.e. $[Q_A^-]_{total}$, $Q_A^-Q_B$, $Q_A^-Q_B^-$, $Q_A^-Q_B^2$, and $Q_A^-Q_BH_2$, curves 1–5 respectively), and the ratio $[PQ](t)/[PQ]_{total}$ (curve 6), are shown in Fig. 4(a). We note that curve 1 also represents the fraction of the closed reaction centres, as the total concentration of the PS II units used in simulation was set to be equal to unity. Similar curves of open reaction centres are shown in the inset: $[Q_A]_{total}$, Q_AQ_B, $Q_AQ_B^-$, $Q_AQ_B^{2-}$, and $Q_AQ_BH_2$, curves 7–11, respectively. It can be seen that at the J step two of the redox states of the closed centres, $Q_A^-Q_B$ and $Q_A^-Q_B^-$, predominate. Although a mixture of different closed forms of PS II centres is present at I and P steps, the $Q_A^-Q_BH_2$ redox state clearly predominates (see curve 5). The fraction of the closed reaction centres (curve 1, $[Q_A^-]_{total} = B$) has a maximal value close to 0.8 in this simulation. The value of B_{max} depends on several factors such as the initial Q_A reduction rate constant, and the rate constant of plastoquinol oxidation (results not shown). It can reach the highest value, $B_{max} = 1$, when the reaction of plastoquinol oxidation is inhibited (Stirbet & Strasser, 1995), which means that the connection between the two photosystems is interrupted.

The PQ pool is mostly reduced in the I–P interval. The degree of PQ pool reduction at steady-state strongly depends on the rate of plastoquinol oxidation (PS I activity). If this rate is zero (blocked PS I), then the PQ pool is completely reduced at the P level.

In Fig. 4(b) the normalised curves of the fraction of the closed reaction centres, $B(t)/B_{max}$, of the unquenched relative variable fluorescence, $V^u(t)/V^u_{max}$, and of the relative variable fluorescence, $V(t)/V_{max}$, are shown. The absolute curves $B(t)$, $V^u(t)$ and $V(t)$ are also shown in the inset. The value of the connectivity parameter used in these simulations was $C = 1$. The normalised fraction of the closed PS II centres, curve $B(t)/B_{max}$ [Fig. 4(b)], has higher values than that of the relative variable fluorescence, $V(t)/V_{max}$, at both the J and I levels. The figure also shows that the PQ quenching phenomenon lowers mainly the I level of the normalised relative variable fluorescence curves.

To understand how different initial parameters of the model could affect the shape of calculated curves, results obtained with different values for several parameters are discussed below.

INITIAL RATIOS OF S_1:S_0 AND Q_B:Q_B^-

The initial concentrations of the reactants are important parameters of the model. We have considered here that initially all PS II units are open (i.e. with Q_A in oxidised state), OEC is either in the S_1 or S_0 state, and Q_B is partially reduced in a fraction of centres (i.e. in Q_B^- state). This is proposed to be the case for dark adapted samples. Therefore, in our model we have four initial concentrations which are different from zero [$S_1Q_AQ_B$ and $S_0Q_AQ_B^-$ from Fig. 3(a); $S_0Q_AQ_B$ and $S_1Q_AQ_B^-$ from Fig. 3(b)]. These values must be chosen to fulfil some specific S_1: S_0 and Q_B:Q_B^- ratios, as reported in the literature for the dark adapted situation (see Table 1—Kok *et al.*, 1970; Forbush *et al.*, 1971; Wollman, 1978; Rutherford *et al.*, 1984). Figure 5(a–f) shows the results of simulation for two values of the S_1:S_0 ratio (1.0:0.0 and 0.8:0.2) and three values of the Q_B:Q_B^- ratio (1.0:0.0, 0.7:0.3, and 0.5:0.5). It can be seen that these different ratios affect both the J and I steps. The J step has higher intensities as the fraction of Q_B^- is increased. The I step has almost the same intensity, but it can be followed by a dip, more or less deep, depending mostly on the Q_B:Q_B^- ratio. The largest dip is observed for the Q_B:Q_B^- ratio of 0.5:0.5 [Fig. 5(c and f)], a small one for 1.0:0.0 [Fig. 5(a and d)], and no dip for 0.7:0.3 [Fig. 5(b and e)]. From the two S_1:S_0

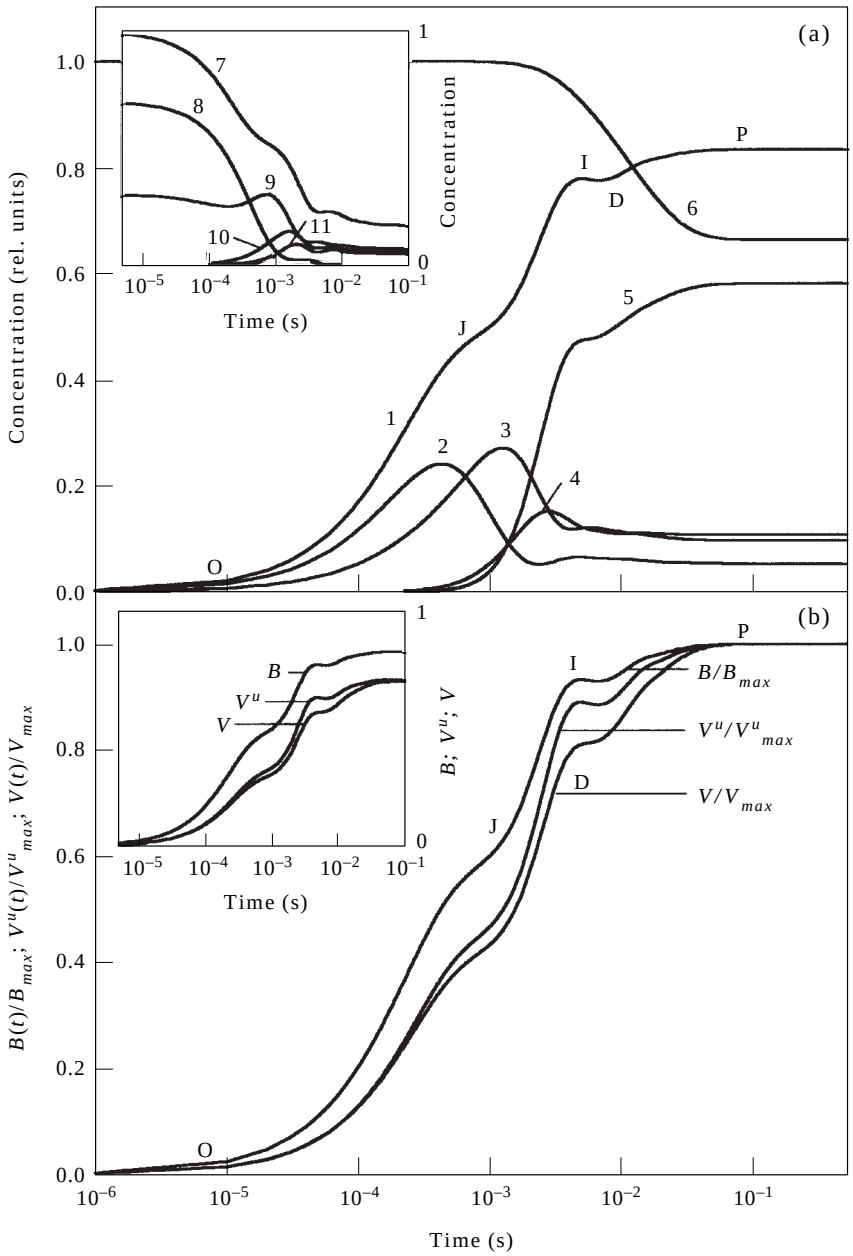

FIG. 4. Typical theoretical curves obtained with our model with input parameters for dark adapted conditions presented in Table 1. (a) Time course of the concentrations of $[Q_A^-]_{total} = B$, $Q_A^-Q_B$, $Q_A^-Q_B^-$, $Q_A^-Q_B^{2-}$, $Q_A^-Q_BH_2$ and $PQ/[PQ]_{total}$ (curves 1–6, respectively); [inset in panel (a)] time course of the concentrations of $[Q_A]_{total}$, Q_AQ_B, $Q_AQ_B^-$, $Q_AQ_B^{2-}$, and $Q_AQ_BH_2$ (curves 7–11, respectively); (b) time course of $B(t)/B_{max}$, $V^u(t)/V^u_{max}$, and $V(t)/V_{max}$—where $B(t)$ is the fraction of closed PS II centres at time t, and B_{max}, is the highest value of $B(t)$; $V^u(t)$ is the unquenched relative variable fluorescence at time t, and V^u_{max}, is the highest value of $V^u(t)$; and $V(t)$ is the PQ-quenched relative variable fluorescence at time t, and V_{max} is the highest value of $V(t)$; [inset in panel (b)] time course of $B(t)$, $V^u(t)$ and $V(t)$. For explanation of the symbols O, J, I, D, and P see the text.

ratios used in the simulations, the ratio of 0.8:0.2 only produced a slight dip. For the ratio $Q_B:Q_B^- = 0.5:0.5$ we have also observed a decrease of approximately 5–10% in the value of the relative variable fluorescence at the P level (results not shown).

In the present paper we have used the initial ratios $S_1:S_0 = 0.8:0.2$ and $Q_B:Q_B^- = 0.7:0.3$ in all the other simulations. We must note that we have chosen the value of 0.7:0.3 for the $Q_B:Q_B^-$ ratio, as reported for isolated chloroplasts (Wollman, 1978), and not 0.5:0.5, as reported for spinach leaves (Rutherford *et al.*, 1984), because normally, the transients in high light of most dark adapted leaves do not show a significant dip.

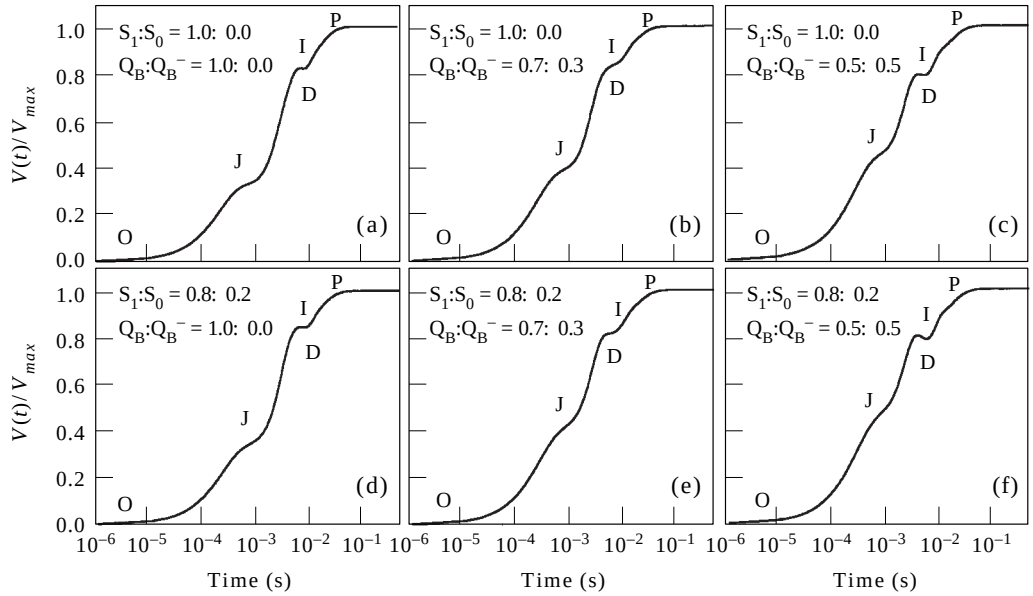

FIG. 5. Simulated Chl *a* fluorescence induction curves ($V(t)/V_{max}$) in dark adapted conditions for different values of initial S_1:S_0 and Q_B:Q_B^- ratios: (a) 1.0:0.0 and 1.0:0.0; (b) 1.0:0.0 and 0.7:0.3; (c) 1.0:0.0 and 0.5:0.5; (d) 0.8:0.2 and 1.0:0.0; (e) 0.8:0.2 and 0.7:0.3; and (f) 0.8:0.2 and 0.5:0.5. For definition of symbols, see the Glossary.

PS II CONNECTIVITY

An important parameter of the present model is the connectivity parameter, C, which depends on the probability of connectivity between the PS II units (see Strasser *et al.*, 1992). C is the constant for the curvature of the hyperbola, V vs. B, derived by Joliot & Joliot (1964) and Strasser (1978) [see eqn (1)]. Figure 6 shows the influence of connectivity on the fluorescence transients of a DCMU treated leaf. We have simulated the fluorescence induction curves for two extreme values of the connectivity parameter (i.e. $C = 0$ and $C = 4$), and for $C = 1$. In the linear time plot, the sigmoidal shape of the simulated curves for $C = 1$ and 4 can be observed. It must be noted that the sigmoidicity of experimental DCMU transients was the first argument that favoured the PS II connectivity concept (Joliot & Joliot, 1964).

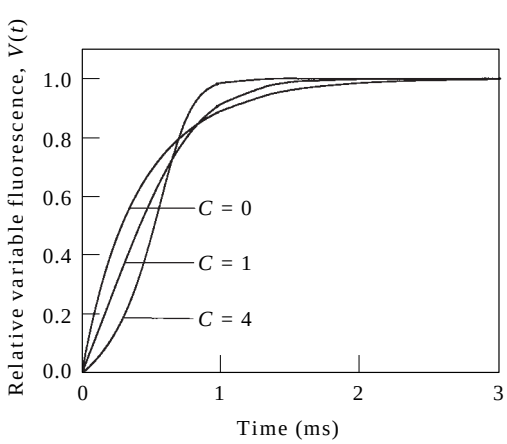

FIG. 6. Simulated Chl *a* fluorescence induction curves in dark adapted conditions (see Table 1) in the presence of DCMU. Relative variable fluorescence curves, $V(t)$, have been calculated at a fixed initial Q_A reduction rate constant, $kL_0^1 = 2000\ s^{-1}$, but with varying connectivity parameter, $C = 0$, 1, and 4.

The effect of the connectivity on the fluorescence transient curves simulated for the untreated dark adapted leaf is presented in Fig. 7(a) and (b). The fraction of closed centres, B [Fig. 7(a)], and the quenched relative variable fluorescence, V [Fig. 7(b)], both normalised at their highest values, have been calculated for various values of the connectivity parameter (i.e. $C = 0$, 1, 1.5, and 2). The absolute curves are presented in the inserts. According to eqn (2) from the theory and assumptions of the model, the Q_A reduction rate (kL) increases with the number of the closed centres, $B(t)$. This increase is more pronounced for larger values of C (e.g. for $C = 1$, the kL value when all centres are closed is doubled compared to that when all centres are open, but for $C = 2$ it is tripled). As a consequence, as the C value increases, an increased number of PS II centres are closed [see Fig. 7(a) inset] due to a higher electron transport rate. However, the relative variable fluorescence decreases with C [see Fig. 7(b) inset], as the connectivity diminishes the loss of trapped energy as fluorescence, favouring a better utilisation of the excitons.

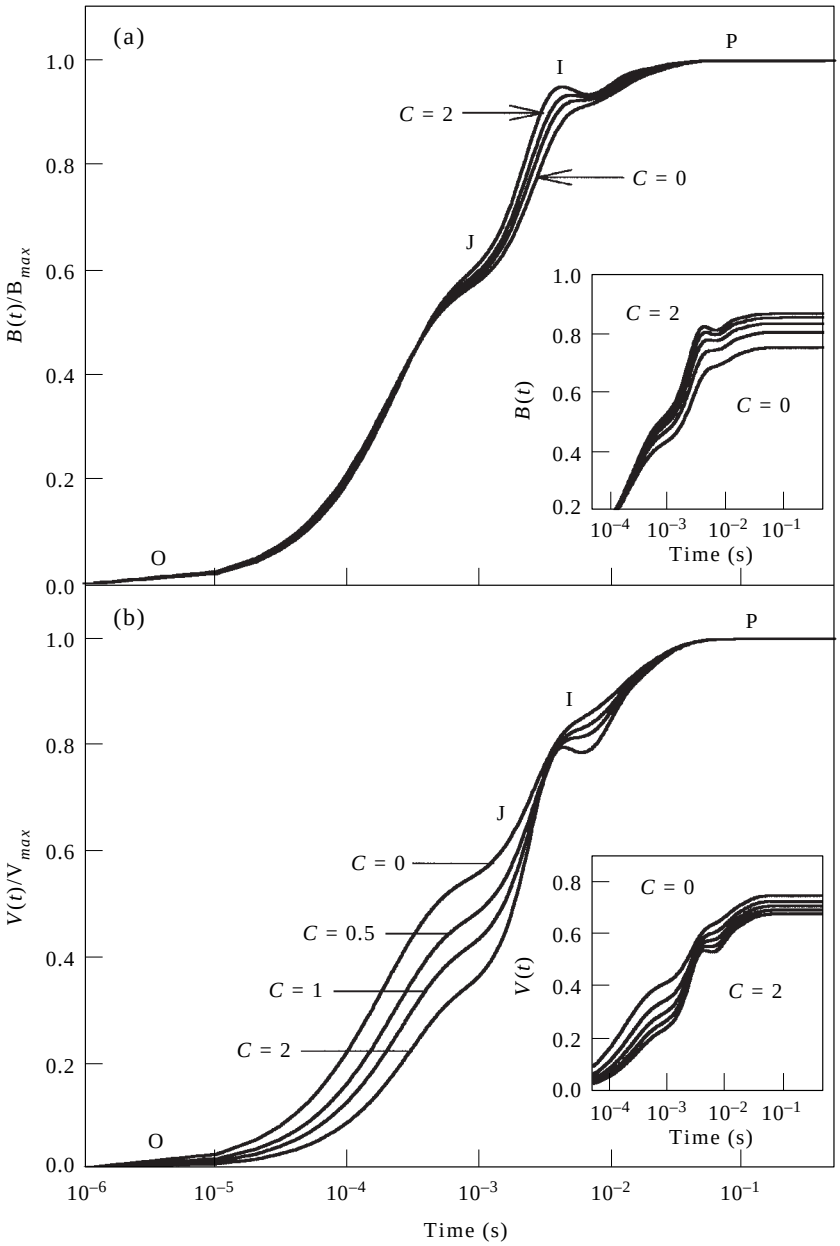

FIG. 7. Simulation results for Chl *a* fluorescence induction obtained in dark adapted conditions (see Table 1), with different values of the connectivity parameter, $C = 0$, 0.5, 1 and 2: (a) time course of $B(t)/B_{max}$; [inset in panel (a)] time course of $B(t)$; (b) time course of $V(t)/V_{max}$; [inset in panel (b)] time course of $V(t)$. For definition of symbols, see the Glossary.

For the normalised fraction of PS II closed centres, B/B_{max} curves, small increases at the I-step can be observed with increasing values of C. For the V/V_{max} curves the J and I steps have lower values as C is increased. As can be seen, the connectivity parameter has much more influence on the normalised relative variable fluorescence curves V/V_{max} than on the B/B_{max} curves.

Since 1964 (Joliot & Joliot) the connectivity of PS II antenna has been measured with fluorescence techniques. According to Paillotin (1976) the quantum yield of the excitation energy trapping by an open reaction centre, $\varphi_{P(t)}$, is:

$$\varphi_{P(t)} = \varphi_{Po}[1 - V(t)] \tag{4}$$

where φ_{Po} is the quantum yield of the excitation energy trapping by an open reaction centre at $t = 0$. Therefore, for steady state conditions and a given light intensity, the electron transport rate is proportional to the relative quantum yield,

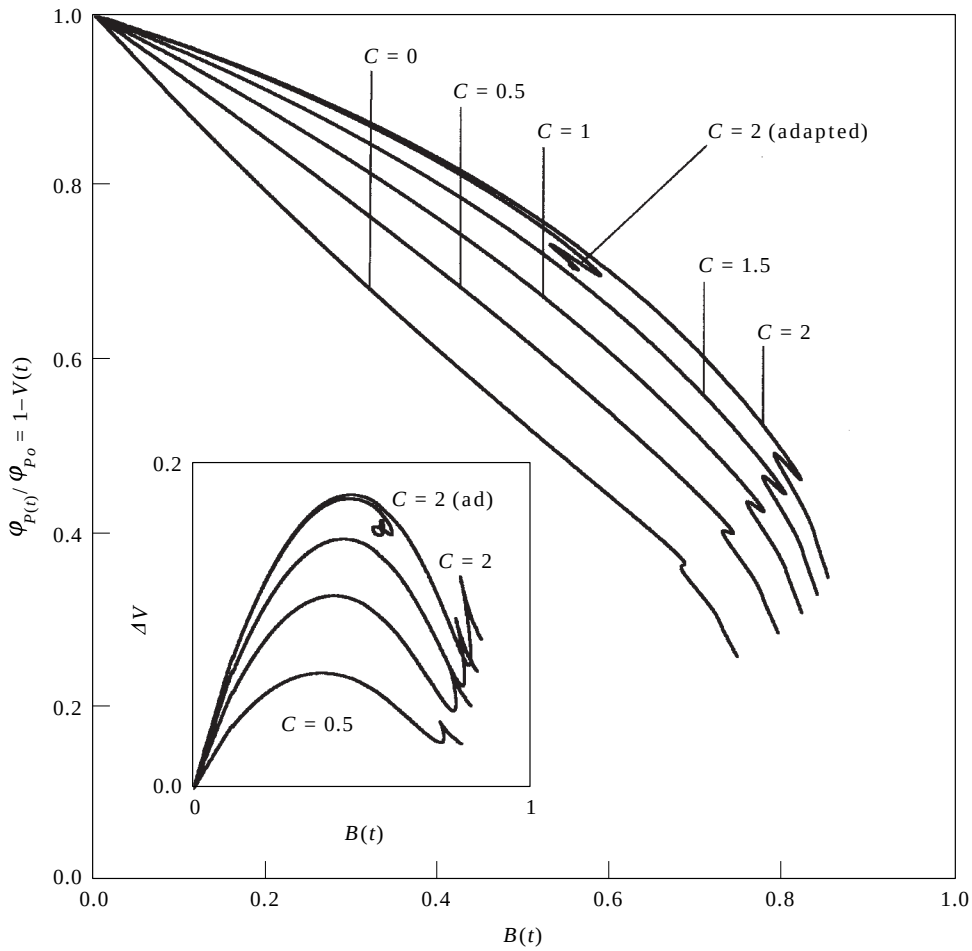

FIG. 8. The relative quantum yield of the exciton energy trapping of an open reaction centre, $1 - V(t)$, as a function of the fraction of closed reaction centres, $B(t)$, for different values of the connectivity parameter, $C = 0$, 0.5, 1, 1.5 and 2; (inset) the differences $\Delta V = [1 - V(t)]_{for\ C \neq 0} - [1 - V(t)]_{for\ C = 0}$ as a function of the fraction of closed reaction centres, $B(t)$, for different values of the connectivity parameter, $C = 0$, 0.5, 1, 1.5 and 2. All the curves are obtained with the input parameters for dark adapted conditions presented in Table 1, except the curve $C = 2$ (adapted) which was obtained with an increased value of the rate constant of plastoquinol oxidation, $k_P = 300\ s^{-1}$ instead of $70\ s^{-1}$, and an increased value of the PQ exchange reaction, $k_E = 1000\ s^{-1}$ instead of $100\ s^{-1}$. For definition of symbols, see the Glossary.

$\varphi_{P(t)}/\varphi_{Po} = 1 - V(t)$. In Fig. 8 the simulated curves $[1 - V(t)]$ vs. $B(t)$ are shown, for different values of the connectivity constant C. It is evident that a higher degree of connectivity produces an increase in the value of $[1 - V(t)]$ and therefore, the value of the electron transport. However, we put forward the hypothesis that the connectivity has also a more qualitative goal: the stability of the system in an optimal state relative to the environmental conditions. The difference of the relative quantum yields between the connected and the unconnected case:

$$\Delta V = [1 - V(t)]_{for\ C \neq 0} - [1 - V(t)]_{for\ C = 0} \qquad (5)$$

is a function with a well defined optimum (see Fig. 8 inset) which is linked to the redox buffering capacity of the system. The numerical simulations made for dark adapted samples show that at steady state the system is far away from the optimum. However, if we consider an "adapted" system (e.g. with an increased value of the rate constant of plastoquinol oxidation, $k_P = 300\ s^{-1}$ instead of $70\ s^{-1}$, and of the PQ exchange reaction, $k_E = 1000\ s^{-1}$ instead of $100\ s^{-1}$) the results show that the system approaches the optimum of this function. A fitting procedure can allow us to determine the best choice of the rate constants, but this will be the objective of another paper. Therefore, we can conclude that the connectivity influences the function of the photosynthetic systems both as activity (the electron transport) and stability of the system towards external perturbations (stress buffering, Krüger *et al.*, 1997).

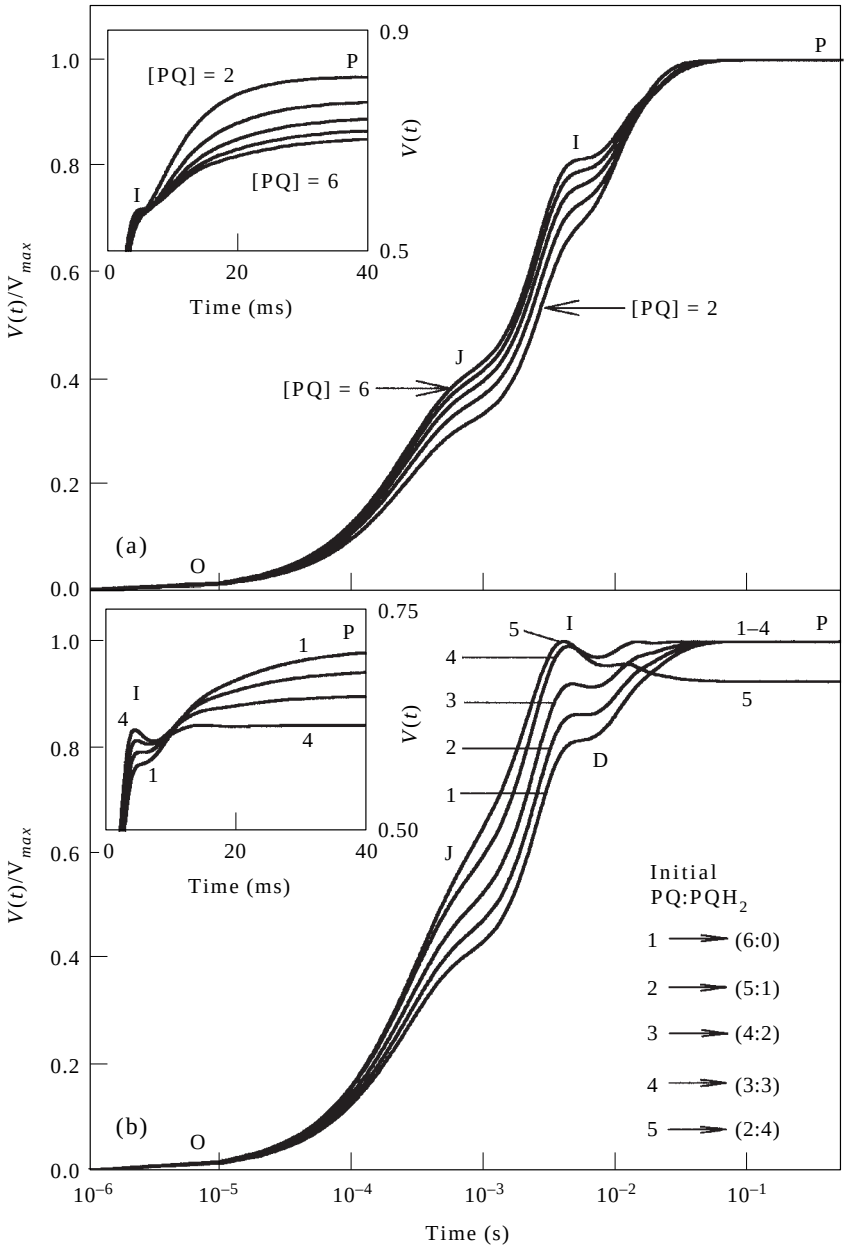

FIG. 9. Simulated Chl *a* fluorescence transients in dark adapted conditions (see Table 1) for: (a and the inset panel) different number of PQ pool molecules: [PQ] = 2, 3, 4, 5 and 6; (b and the inset panel) different degree of PQ pool oxidation: $PQ:PQH_2$ = 6:0, 5:1, 4:2, 3:3 and 4:2, (curves 1–5, respectively). For definition of symbols, see the Glossary.

PQ POOL

The relative variable fluorescence curves simulated for different number of plastoquinone molecules in the pool are shown in Fig. 9(a). As the plastoquinone exchange reaction is a second order reaction, the rate constant of this reaction, k_E, depends on the half time, ${}^2t_{1/2}$, and the number of PQ pool molecules that are initially in the oxidised state, $k_E = \ln 2/({}^2t_{1/2}[PQ]_0)$. In these simulations we have used the value for the half time of the PQ exchange reaction to be 1 ms, independent of the number of the PQ molecules in the pool. It can be seen that the number of PQ molecules in the pool changes the shape of the $V(t)/V_{max}$ curves, especially in the J–I domain. However, the absolute values of the relative variable fluorescence, $V(t)$, are changed largely in the I–P domain: the greater the number of PQ molecules in the pool, the lesser the steady state value of V (e.g. at step P, $V(t)/_{PQ=2} \cong 0.8$ and $V(t)/_{PQ=6} \cong 0.7$—a decrease of $\sim 14\%$) [Fig. 9(a) inset]. At the same time, the steady-state value of the

fraction of closed centres $B(t)$ at P decreases by ~8% as the number of PQ molecules in the pool increases from two to six (results not shown). It is obvious that the number of PQ pool molecules per PS II centre in the sample is very important for the fitting of the model with experimental data. As was shown earlier (Lavergne *et al*., 1992; Hsu, 1992), there is a high probability that the number of PQ molecules which serve one PS II unit is not the same for all PS II. However, we do not consider the PS II and PQ heterogeneity in the present work (see the second assumption of the model).

It must also be noted, that the area over the fluorescence curve in the linear plot is proportional to the number of PQ pool molecules, in agreement with literature predictions (Malkin & Kok, 1966) [see the inset in Fig. 9(a)].

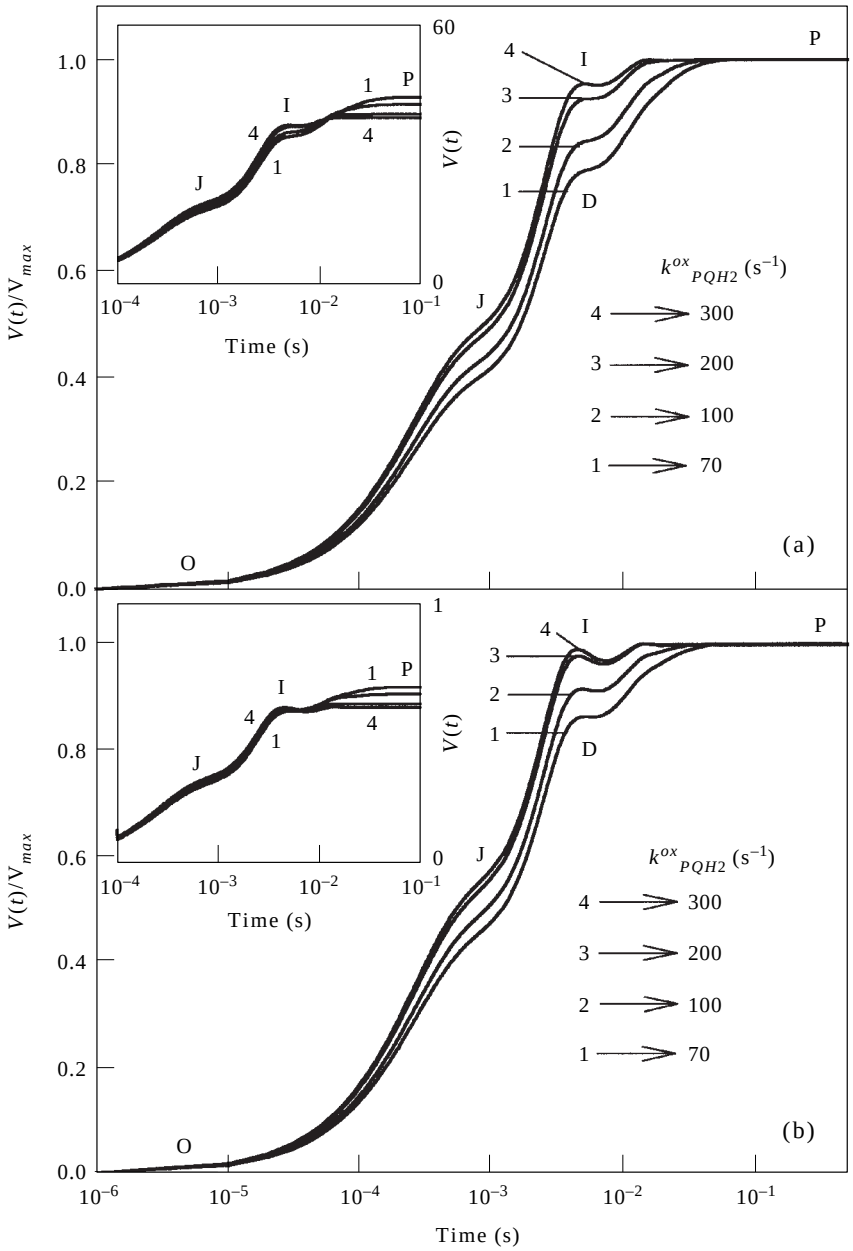

FIG. 10. Simulated Chl *a* fluorescence induction for dark adapted conditions (see Table 1) for different values of the plastoquinol oxidation rate constant, $k^{ox}_{PQH2} = 70$, 100, 200 and 300 s^{-1} (curves 1–4, respectively). (a and the inset panel) considering five molecules in PQ pool, all oxidised initially; (b and the inset panel) considering six molecules in PQ pool, initially five oxidised and one reduced. For definition of symbols, see the Glossary.

REDOX STATE OF THE PQ POOL

Figure 9(b) shows the results obtained for a PQ pool of six molecules with different initial $PQ:PQH_2$ ratios (6:0; 5:1; 4:2; 3:3; and 2:4). In all cases we have used the same value of the rate constant, $k_E = 115.5\ s^{-1}$ (resulting from ${}^2t_{1/2} = 1$ ms, and $[PQ]_0 = 6$). The transients change dramatically in both the J–I and I–P domains (see also the inset). As the initial PQH_2 concentration increases, the I value of the relative variable fluorescence $V(t)$ becomes higher, and P value smaller. In the curve simulated for $PQ:PQH_2 = 2:4$ the maximum level is already reached by the I step and is followed by a subsequent decline [see Fig. 9(b) curve 5]. At the steady state (step P), as the initial PQH_2 concentration increases from zero to four, the PQ concentration and the fraction of closed PS II centres decrease by ~ 8 and $\sim 11\%$, respectively (results not shown).

RATE OF PLASTOQUINOL OXIDATION

The transients simulated for different values of the plastoquinol oxidation rate constant are presented in Fig. 10. This reaction takes place at the Cyt b/f level (Hauska *et al*., 1996) which is connected to the PS I centres by the soluble electron carrier plastocyanin (see Fig. 2). Therefore, the ratio between the rate constants of PQH_2 oxidation (k^{ox}_{PQH2}) and Q_A reduction (kL) will reflect the balance between the two photosystems. In Fig. 10 the curves obtained with different plastoquinol oxidation rate constants ($k^{ox}_{PQH2} = 70$, 100, 200, and $300\ s^{-1}$) but with the same initial value of the Q_A reduction rate constant ($kL^0_1 = 2000\ s^{-1}$) are shown. In Fig. 10(a) we have considered a PQ pool with five molecules, initially all oxidised, and in Fig. 10(b) a PQ pool with six PQ molecules, among which five are initially oxidised and one is reduced. In both cases, for higher PQH_2 oxidation rates, the relative variable fluorescence increases at the I and J steps and decreases at the P step (see Fig. 10 insets). Moreover, the P level is reached more rapidly for high values of the plastoquinol oxidation rate constant. The differences observed in the results presented in Fig. 10(a) and10(b) will be discussed below.

ON THE APPEARANCE OF A DIP "D"

As can be seen in several of the presented figures, the model predicts in certain conditions the appearance of a descending phase between the I and P steps. The results show that there are several factors which influence its appearance. Firstly, it must be pointed out that the dip D does not appear in the simulations from the models based only on the reactions from the acceptor side of PS II (Renger & Schulze, 1985; Baake & Strasser, 1990; Baake & Schlöder, 1992; Hsu, 1992, 1993; Stirbet & Strasser, 1995). We have obtained this dip only on considering the states S_n of OEC in the model. However, we have shown that although this is a necessary condition, it is not sufficient. The other properties of the system also influence it. The dip D appears and becomes deeper when: (1) the initial $Q_B:Q_B^-$ ratio of PS II centres is close to 0.5:0.5 [Fig. 5(f)]; (2) the number of the molecules in the PQ pool is increased [Fig. 9(a)]; (3) the initial number of reduced molecules, PQH_2, in the pool is increased [Fig. 9(b)]; and (4) the rate constant of plastoquinol oxidation is increased (Fig. 10). In the last case, the dip is more pronounced if the PQ pool is initially partially reduced (Fig. 10(b)]. These results are in agreement with the interpretation of the dip as being mainly related to the dynamic equilibrium between the functioning of the two photosystems (see Munday & Govindjee, 1969; Schreiber & Vidaver, 1974).

TRANSIENTS OF LIGHT-ADAPTED LEAVES

A further test of the present model would be achieved if we could simulate the results obtained in experiments in which some external parameters are varied. Here, we have chosen to test the model by simulating transients of light adapted plants (Strasser *et al*., 1995; Stirbet *et al*., 1995).

In the light-adapted conditions (see Material and Methods for the experimental conditions) we have assumed that: (1) initially the PQ pool is partially reduced ($PQ:PQH_2 = 4:2$); (2) the degree of connectivity between PS II units is smaller than for dark adapted conditions ($C = 0.25$ instead of 1.00); and (3) the initial rate constant of Q_A reduction has a lower value, $kL^0_1 = 1000\ s^{-1}$ instead of $2000\ s^{-1}$, as in short-term adaptation strategies of plants the absorbed light energy is assumed to be dissipated as heat to a greater extent (Staehelin & van der Staay, 1996). In Fig. 11 the curves 1 and 2 are the transients simulated for dark and light adapted conditions, respectively. It can be observed that in the light adapted conditions the relative variable fluorescence reaches its maximum value at the I level (P = I), just as in the experimental data (see the inset in Fig. 11—curves 1 and 2 obtained using experimental data presented in Strasser *et al*., 1995). Whether or not this is a unique solution remains to be proven. The above provides a method for testing and provides a means to quantitate and to predict fluorescence transients under various conditions, with known reactions and rate constants in PS II.

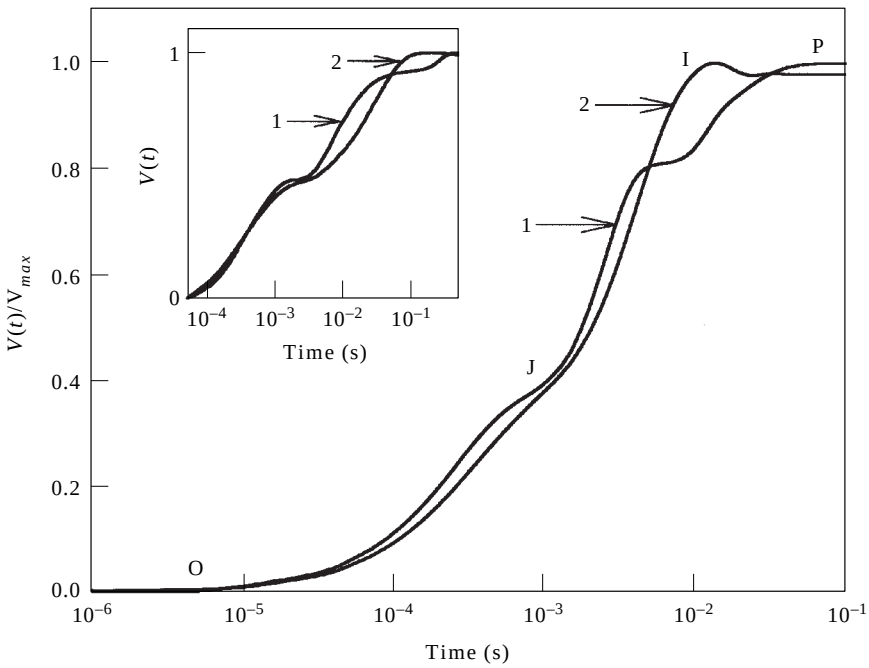

FIG. 11. Time course of the variable Chl *a* fluorescence induction, $V(t)/V_{max}$, simulated with input parameters corresponding to the dark adapted and light adapted conditions (see Table 1) (curves 1 and 2, respectively). In the inset, the curves obtained with experimental data presented in Strasser *et al*. (1995) are shown. For definition of symbols, see the Glossary.

Conclusions

The mathematical model of the first phase of Chl *a* fluorescence induction in plants presented here utilises the redox reactions at both the acceptor and donor sides of PS II [see Figs 2 and 3(a) and (b)]. The consistency of the model is supported by the fact that the rate constants of the reactions used in simulations have values close to those reported in the literature (see Table 1). The global rate of reduction of Q_A was considered to include the light reaction in the model, and we have assumed that its value is two times higher in the S_0 and S_1 states than in the S_2 and S_3 states. Partial connectivity between PS II units [see eqns (1)–(3), and PQ non-photochemical quenching (see Appendix) were also needed to explain the experimental data. The simulated fluorescence transient parallel the characteristic O–J–I–P steps observed in experimental transients. According to this model, the polyphasic O–J–I–P shape of the induction curve is due to the dynamic variations of the concentrations of various redox states of PS II units [see Fig. 4(a)]. At the J step, $Q_A^- Q_B$ and $Q_A^- Q_B^-$ states predominate. A mixture of different closed states of PS II units is present at the I and P steps, the $Q_A^- Q_B H_2$ state having the highest concentration.

The simulation presented in Fig. 4 shows that even with high light intensity the PS II units are not all in the closed state when the maximum fluorescence yield is attained, as the reoxidation of PQH_2 by PS I is active. Only in the case of PS I inhibition can the fraction of PS II closed centres reach the maximum value, $B = 1$.

It was shown that the connectivity between PS II antenna influences the function of the photosynthetic systems both quantitatively (enhancing the electron transport) and qualitatively (increasing the stability) (see Fig. 8). The connectivity parameter between PS II units strongly modifies the shape of the normalised relative variable fluorescence curve, mainly by slowing down the O–J phase [see Figs 4(b) and 7(b)].

The PQ non-photochemical quenching affects in particular the I step of the normalised transient, decreasing its value [see Fig. 4(b)].

The number of plastoquinone molecules per PS II centre was assumed to be identical for all the centres in this current model (i.e. a homogeneous distribution of PQ). This, of course, does not challenge the existence of heterogeneity (Melis & Homann, 1975). The simulated transients obtained with different number of molecules in the PQ pool have modified shapes, especially in the I–P region [Fig. 9(a) inset]. We have shown that the relationship between the complementary area of the fluorescence transient and the number of plastoquinone molecules is still valid when non-photochemical quenching by the PQ-pool is considered. Moreover, the model predicts that the

initial degree of PQ pool oxidation also influences the transient [Fig. 9(b)].

The ratio between PS II and PS I activity, expressed here as the ratio between the rate constants of Q_A reduction and PQH_2 oxidation, also strongly influences the transient. The relative variable fluorescence intensity at the J and I steps increases as the activity of PS I is accelerated, and for high PS I activity (i.e. plastoquinol oxidation rate constant $>300\ s^{-1}$) it can reach its maximum value as early as the I level [Fig. 10(b)]. At the same time, the P step decreases with the increase of PS I activity (Figs 9 and 10 insets).

The results presented here show that in certain conditions, a descending region of the curve appears between the I and P steps, usually denoted as dip D. It was not possible to simulate this dip with any of the models that use only the acceptor side of PS II. Therefore, we can conclude that it is mainly due to the S_n states. However, this dip is also influenced by many other factors, such as the ratio between the rates of PS II and PS I activities, the degree of PS II connectivity, the initial Q_B:Q_B^- ratio, the number of molecules in the PQ pool, and the initial number of oxidised plastoquinone molecules in the pool. The dip is more pronounced when the relative activity of PS I is increased, the connectivity parameter C is higher, the initial value of the Q_B:Q_B^- ratio is close to 0.5:0.5, the number of molecules in the PQ pool is higher, and the initial number of oxidised plastoquinone molecules in the pool is higher.

The simulated curves of fluorescence induction of the light adapted plants exhibit, as in the experimental ones, only the O, J, and I(=P) levels (Fig. 11).

In conclusion, the model presented here allows the possibility to obtain quantitative information from fluorescence transients of leaves, regarding the individual PS II reactions and the interaction of PS II with PS I, which are often difficult to measure directly. The simulations also take into account the donor side of PS II and the non-photochemical quenching by PQ, until now neglected. The next step to be achieved in this work is to provide the fitting of experimental data with the theoretical data obtained through numerical simulation, in order to calculate the values of the input parameters of the model. We expect to establish in this way, data banks for the enormous amount of samples being measured in ecological and environmental investigations.

We thank Alaka Srivastava for the experimental data on fluorescence transients of light-adapted leaves used in this paper, and Merope Tsimilli for helpful discussions. This work was supported by Swiss National Foundation (Grant No. 3100-046860.96/1).

REFERENCES

Baake, E. & Schlöder, J. P. (1992). Modeling the fast fluorescence rise of photosynthesis. *Bull. Math. Biol.* **54,** 999–1021.

Baake, E. & Strasser, R.J. (1990). A differential equation model for the description of the fast fluorescence rise (O–I–D–P-transient) in leaves. In: *Current Research in Photosynthesis*, Vol. 1 (Baltscheffsky, M., ed.), pp. 567–570. The Netherlands: Kluwer Academic Publisher.

Babcock, G.T. (1987). The photosynthetic oxygen-evolving process. In: *New Comprehensive Biochemistry*, *Vol.* 15, *Photosynthesis* (Amesz, J., ed.), pp. 125–158. Amsterdam: Elsevier.

Babcock, G. T., Blankenship, R. E. & Sauer, K. (1976). Reaction kinetics for positive charge accumulation on the water side of chloroplast photosystem II. *FEBS Lett.* **61,** 286–289.

Bouges-Bocquet, B. (1973). Electron transfer between the two photosystems in spinach chloroplasts. *Biochim. Biophys. Acta* **314,** 250–256.

Britt, R. D. (1996). Oxygen evolution. Structure, dynamics, and energy conversion efficiency in photosystem II. In: *Advances in Photosynthesis*, *Vol.* 4, *Oxygenic Photosynthesis*: *The Light Reactions* (Ort, D. R. &. Yocum, C. F., eds), pp. 137–164. The Netherlands: Kluwer Academic Publishers.

Butler, W. L. (1972). On the primary nature of fluorescence yields changes associated with photosynthesis. *Proc. Natl. Acad. Sci. U.S.A.* **69,** 3420–2422.

Butler, W. L. (1978). Energy distribution in the photochemical apparatus of photosynthesis. *Ann. Rev. Plant Physiol.* **29,** 345–378.

Butler, W. L. (1980). Energy transfer between Photosystem II units in a connected package model of the photochemical apparatus of photosynthesis. *Proc. Natl. Acad. Sci. U.S.A.* **77,** 4697–4701.

Crofts, A. R. & Wraight, C. A. (1983). The electrochemical domain of photosynthesis. *Biochim. Biophys. Acta* **726,** 149–185.

Crofts, A. R., Robinson, H. H. & Snozzi, M. (1984). Reactions of quinols at catalytic sites; a diffusional role in H-transfer. In: *Advances in Photosynthesis Research*, Vol. 1 (Sybesma, C., ed.), pp. 461–468. The Hague: Martinus Nijhoff/Dr. W. Junk.

Dau, H. (1994). Molecular mechanisms and quantitative models of variable photosystem II fluorescence. *Photochem. Photobiol.* **60,** 1–23.

Delosme, R. (1971). New results about chlorophyll fluorescence "in vitro". In: *Proceedings of the 2nd International Congress on Photosynthesis Research* (Forti, G., Avron, M. & Melandri, A., eds), pp. 187–195. The Netherlands: W. Junk.

Deprez, J., Dobek, A., Geacintov, N. E., Paillotin, G. & Breton, J. (1983). Probing fluorescence induction in chloroplasts on a nanosecond time scale utilizing picoseconde laser pulse pairs. *Biochim. Biophys. Acta* **752,** 444–454.

Diner, B. A. (1977). Dependence of the deactivation reactions of Photosystem II on the redox state of the plastoquinone pool A, varied under anaerobic conditions. Equilibria on the acceptor side of Photosystem II. *Biochim. Biophys. Acta* **460,** 247–258.

Diner, B. A. & Babcock, G. T. (1996). Structure, dynamics, and energy conversion efficiency in photosystem II. In: *Advances in Photosynthesis Vol.* 4, *Oxygenic Photosynthesis*: *The Light Reactions* (Ort, D. R. & Yocum, C. F., eds), pp. 213–247. The Netherlands: Kluwer Academic Publishers.

Duysens, L. M. N. & Sweers, H. E. (1963). Mechanism of the two photochemical reactions in algae as studied by means of fluorescence. In: *Studies on Microalgae and Photosynthetic Bacteria* (Japanese Society of Plant Physiologists, ed.), pp. 353–372. Tokyo: University of Tokyo Press.

Forbush, B., Kok, B. & McGloin, M. P. (1971). Cooperation of charges in photosynthetic O_2 evolution. II. Damping of flash yield oscillations deactivation. *Photochem. Photobiol.* **14,** 307–321.

Fork, D. C. & Mohanty, P. (1986). Fluorescence and other characteristics of blue-green algae (cyanobacteria), red algae, and cryptomonads. In: *Light Emission by Plants and Bacteria* (Govindjee, Amesz, J. & Fork, D. C., eds), pp. 451–496. New York: Academic Press.

Govindjee (1995). Sixty-three years since Kautsky: chlorophyll *a* fluorescence. *Aust. J. Plant Physiol.* **22,** 131–160.

Govindjee & Papageorgiou, G. (1971). Chlorophyll fluorescence and photosynthesis: fluorescence transients. *Photophysiology* **6,** 1–50.

Greenfield, S. & Wasielewski, M. R. (1996). Excitation energy transfer and charge separation in the isolated Photosystem II reaction center. *Photosynth. Res.* **48,** 83–97.

Haehnel, W. (1984). Photosynthetic electron transport in higher plants. *Ann. Rev. Plant. Physiol.* **35,** 659–693.

Hansson, O. & Wydrzynski, T. (1990). Current perceptions of photosystem II. *Photosynth. Res.* **23,** 131–162.

Hauska, G., Schütz, M. & Büttner, M. (1996). The cytochrome b_6f complex—composition, structure and function. In: *Advances in Photosynthesis. Vol. IV. Oxygenic Photosynthesis: The Light Reactions* (Ort, D. R. & Yocum, C. F., eds), pp. 377–398. The Netherlands: Kluwer Academic Publishers.

Hindmarsch, A. C. (1980). LSODE and LSOI, two initial value of ordinary differential equation solvers. *A.C.M. Signum Newsletter*, **15,** 10–11.

Hsu, B.-D. (1992). A theoretical study on the fluorescence induction curve of spinach thylakoids in the absence of DCMU. *Biochim. Biophys. Acta* **1140,** 30–36.

Hsu, B.-D. (1993). Evidence for the contribution of the S-state transitions of oxygen evolution to the initial phase of fluorescence induction. *Photosynth. Res.* **36,** 81–88.

Hsu, B.-D., Lee, Y.-S. & Jang, I.-R. (1989). A method for analysis of fluorescence induction curve from DCMU-poisoned chloroplasts. *Biochim. Biophys. Acta* **975,** 44–49.

Joliot, A. & Joliot, P. (1964). Étude cinétique de la réaction photochimique libérant l'oxygène au cours de la photosynthèse. *C.R. Acad. Sci. Paris* **258,** 4622–4625.

Joliot, P., Bennoun, P. & Joliot, A. (1973). New evidence supporting energy transfer between photosynthetic units. *Biochim. Biophys. Acta* **305,** 317–328.

Joliot, P., Joliot, A., Bouges, B. & Barbieri, G. (1971). Studies of system II photocentres by comparative measurements of luminescence, fluorescence, and oxygen emission. *Photochem. Photobiol.* **14,** 287–305.

Joshi, M. K. & Mohanty, P. (1995). Probing photosynthetic performance by chlorophyll *a* fluorescence: analysis and interpretation of fluorescence parameters. *J. Sci. Ind. Res.* **54,** 155–174.

Karukstis, K. K., Moision, R. M., Johansen, S. K., Birkeland, K. E. & Cohen, S. M. (1992). Alternative measure of photosystem II electron transfer inhibition in anthraquinone-treated chloroplasts. *Photochem. Photobiol.* **55,** 125–132.

Kautsky, H. & Hirsch, A. (1931). Neue Versuche zur Kohlensäuereassimilation. *Natürwissenschaften* **48,** 964.

Kok, B., Forbush, B. & McGloin, M. (1970). Cooperation of charges in photosynthetic oxygen evolution. I—A linear four-step mechanism. *Photochem. Photobiol.* **11,** 457–475.

Krause, G. H. & Weis, E. (1991). Chlorophyll fluorescence and photosynthesis: the basics. *Ann. Rev. Plant. Physiol. Plant. Mol. Biol.* **42,** 313–349.

Krüger, H. J., Tsimilli-Michael, M. & Strasser, R. J. (1997). Light stress provokes plastic and elastic modifications in structure and function of photosystem II in camellia leaves. *Physiol. Plantarum* **101,** 265–277.

Lakowicz, J. R. (1983). Quenching of fluorescence. In: *Principles of Fluorescence Spectroscopy*, Chap. 9, pp. 258–301. New York: Plenum Press.

Latimer, P., Bannister, T. T. & Rabinowitch, E. (1956). Quantum yields of fluorescence of plant pigments. *Science* **124,** 585–586.

Lavergne, J. & Leci, E. (1993). Properties of inactive photosystem II centres. *Photosynth. Res.* **35,** 323–343.

Lavergne, J. & Trissl, H.-W. (1995). Theory of fluorescence induction in photosystem II: derivation of analytical expressions in a model including exciton-radical-pair equilibrium and restricted energy transfer between photosynthetic units. *Biophys. J.* **68,** 2474–2492.

Lavergne, J., Bouchaud, J.-P. & Joliot, P. (1992). Plastoquinone compartimentation in chloroplasts. II—Theoretical aspects. *Biochim. Biophys. Acta* **1101,** 13–22.

Lehrer, S. S. (1971). Solute perturbation of protein fluorescence. Quenching of the tryptophyl fluorescence of model compounds and of lysozime by iodine ion. *Biochemistry* **10,** 3254–3263.

Malkin, S. & Kok, B. (1966). Fluorescence induction studies in isolated chloroplasts. I—Number of components involved in the reaction and quantum yields. *Biochim. Biophys. Acta* **126,** 413–432.

Melis, A. & Homann, P. H. (1975). Kinetic analysis of the fluorescence induction in DCMU poisoned chloroplasts. *Photochem. Photobiol.* **21,** 431–437.

Munday, J. C., Jr. & Govindjee (1969). Light induced changes in the fluorescence yield of chlorophyll *a in vivo*. III—The dip and the peak in the fluorescence transient of *Chlorella pyrenoidosa*. *Biophys. J.* **9,** 1–21.

Neubauer, C. & Schreiber, U. (1987). The polyphasic rise of chlorophyll fluorescence upon onset of strong continuous illumination: I—Saturation characteristics and partial control by the photosystem II acceptor side. *Z. Naturforsch.* **42c**, 1246–1254.

Paillotin, G. (1976). Movement of excitation in the photosynthesis domain of photosystem II. *J. theor. Biol.* **58,** 237–252.

Papageorgiou, G. (1975). Chlorophyll fluorescence: an intrinsic probe of photosynthesis. In: *Bioenergetics of Photosynthesis* (Govindjee, ed.), pp. 319–371. New York: Academic Press.

Renger, G. (1993). Water cleavage by solar radiation—an inspiring challenge of photosynthesis research. *Photosynth. Res.* **38,** 229–247.

Renger, G. & Schulze, A. (1985). Quantitative analysis of fluorescence induction curves in isolated spinach chloroplasts. *Photobiochem. Photobiophys.* **9,** 79–87.

Robinson, H. H. & Crofts, A. R. (1983). Kinetics of the oxidation-reduction reactions of the Photosystem II quinone acceptor complex, and the pathway for deactivation. *FEBS Lett.* **153,** 221–226.

Rutherford, A. R., Govindjee & Inoue, Y. (1984). Charge accumulation and photochemistry in leaves studied by thermoluminiscence and delayed light emission. *Proc. Natl. Acad. Sci. U.S.A.* **81,** 1107–1111.

Schreiber, U. & Bilger, W. (1993). Progress in chlorophyll fluorescence research: major developments during the past years in retrospect. *Prog. Bot.* **54,** 151–173.

Schreiber, U. & Vidaver, W. (1974). Chlorophyll fluorescence induction in anaerobic *Scenedesmus obliquus*. *Biochim. Biophys. Acta* **368,** 97–112.

Shinkarev, V. P. & Govindjee (1993). Insight into the relationship of chlorophyll *a* fluorescence yield to the concentration of its natural quenchers in oxygenic photosynthesis. *Proc. Natl. Acad. Sci. U.S.A.* **90,** 7466–7469.

Seibert, M. (1993). Biochemical, biophysical and structural characterisation of the isolated photosystem II reaction center complex. In: *The Photosynthetic Reaction Center*, Vol. 1 (Deisenhofer, J. & Norris, J., eds), pp. 319–356. New York: Academic Press.

Sonneveld, A., Rademaker, H. & Duysens, L. N. M. (1979). Chlorophyll *a* fluorescence as a monitor of nanosecond reduction of the photooxidized primary donor $P680^+$ of photosystem II. *Biochim. Biophys. Acta* **548,** 536–551.

Srivastava, A., Strasser, R. J. & Govindjee (1995a). Differential effects of dimethylbenzoquinone and dichlorobenzoquinone on chlorophyll fluorescence transient in spinach thylakoid. *J. Photochem. Photobiol.* **31,** 163–189.

Srivastava, A., Strasser, R. J. & Govindjee (1995b). Polyphasic rise of chlorophyll *a* fluorescence in herbicide-resistant D1 mutants of *Chlamidomonas reinardtii*. *Photosynth. Res.* **43,** 131–141.

STAEHELIN, L. A. & VAN DER STAAY, G. W. M. (1996). Structure, composition, functional organization and dynamic properties of thylakoid membranes. In: *Advances in Photosynthesis*. *Vol*. 4. *Oxygenic Photosynthesis*: *The Light Reactions* (Ort, D. R. & Yocum, C. F., eds), pp. 11–30. The Netherlands: Kluwer Academic Publishers.

STIEHL, H. H. & WITT, H. T. (1969). Quantitative treatment of the function of plastoquinone in photosynthesis. *Z*. *Naturforsch*. **24B,** 1588–1598.

STIRBET, A. D. & STRASSER, R. J. (1995). Numerical simulation of the fluorescence induction in plants. *Archs*. *Sci*. *Genève* **48,** 41–60.

STIRBET, A. D. & STRASSER, R. J. (1996). Numerical simulation of the *in vivo* fluorescence in plants. *Math*. *Comp*. *Simulations* **42,** 245–253.

STIRBET, A. D., GOVINDJEE, STRASSER, B. J. & STRASSER, R. J. (1995). Numerical simulation of chlorophyll *a* fluorescence induction in plants. In: *Photosynthesis*: *from Light to Biosphere*, Vol. 2 (Mathis, P., ed.), pp. 919–922. The Netherlands: Kluwer Academic Publishers.

STRASSER, R. J. (1978). The grouping model of plant photosynthesis. In: *Chloroplast Development* (Akoyunoglou, G. *et al*., eds), pp. 513–524. The Netherlands: Elsevier.

STRASSER, R. J. (1981). The grouping model of plant photosynthesis: heterogeneity of photosynthetic units in thylakoids. In: *Structure and Molecular Organization of the Photosynthetic Apparatus* (Akoyunoglou, G., ed.), pp. 727–737. Philadelphia: Balaban International Science Service.

STRASSER, R. J. & GOVINDJEE (1991). The F_0 and the O–J–I–P fluorescence rise in higher plants and algae. In: *Regulation of Chloroplast Biogenesis* (Argyroudi-Akoyunoglou, J. H., ed.), pp. 423–426. New York: Plenum Press.

STRASSER, R. J. & GOVINDJEE (1992). On the O–J–I–P fluorescent transient in leaves and D1 mutants of *Chlamydomonas reinhardtii*. In: *Research in Photosynthesis*, Vol. 2 (Murata, N., ed.), pp. 20–32. The Netherlands: Kluwer Academic Publishers.

STRASSER, R. J., EGGENBERG, P. & GOVINDJEE (1992). An equilibrium model for electron transfer in photosystem II acceptor complex: an application to *Chlamidomonas reinhardtii* cells of D1 mutants and those treated with formate. *Archs*. *Sci*. *Genève* **45,** 207–224.

STRASSER, R. J, SRIVASTAVA, A. & GOVINDJEE (1995). Polyphasic chlorophyll *a* fluorescence transient in plants and cyanobacteria. *Photochem*. *Photobiol*. **61,** 32–42.

TRISSL, H.-W. & LAVERGNE, J. (1994). Fluorescence induction from photosystem II: analytical equations for the yields of photochemistry and fluorescence derived from analysis of a model including exciton radical pair equilibrium and restricted energy transfer between photosynthetic units. *Austr*. *J*. *Plant Physiol*. **22,** 183–193.

TRISSL, H.-W., GAO, Y. & WULF, K. (1993). Theoretical fluorescence induction curves derived from coupled differential equations describing the primary photochemistry of photosystem II by an exciton-radical pair equilibrium. *Biophys*. *J*. **64,** 974–988.

VELTHUYS, B. R. (1981). Electron-dependent competition between plastoquinone and inhibitors for binding to photosystem II. *FEBS Lett*. **126,** 277–281.

VELTHUYS, B. R. & AMESZ, J. (1974). Charge accumulation at the reducing side of system 2 of photosynthesis. *Biochim*. *Biophys*. *Acta* **325,** 138–148.

VERNOTTE, C., ETIENNE, A.-L. & BRIANTAIS, J.-M. (1979). Quenching of the system II chlorophyll fluorescence by the plastoquinone pool. *Biochim*. *Biophys*. *Acta* **545,** 519–527.

WOLLMAN, F. A. (1978). Determination and modification of the redox state of the secondary acceptor of photosystem II in the dark. *Biochim*. *Biophys*. *Acta* **503,** 263–273.

APPENDIX

The experimentally measured relative variable Chl *a* fluorescence is affected by the PQ pool; oxidised PQ pool molecules quench antenna Chl *a* fluorescence (Vernotte *et al*., 1979). Below, we deduce a relationship between the quenched, $V(t)$, and the unquenched, $V^u(t)$, relative variable fluorescence.

The main assumption is that Chl *a* fluorescence quenching induced by oxidised plastoquinones from the PQ pool obeys the Stern–Volmer relationship (Lehrer, 1971; Vernotte, 1979; Lakowicz, 1983; Karukstis *et al*., 1992; Lavergne & Leci, 1993, Srivastava *et al*., 1995a). For a homogeneous population of fluorescence centres that shares the same PQ pool we can write:

$$\frac{F^u(t)}{F(t)} = 1 + K[PQ](t), \tag{A.1}$$

where $F^u(t)$ is the unquenched fluorescence, $F(t)$ is the quenched fluorescence, $[PQ](t)$ is the oxidised plastoquinone concentration, all at the time t, and K is the Stern–Volmer quenching constant of that PS II population. Experimental results (Vernotte *et al*., 1979; Srivastava *et al*., 1995a) have shown that the value of K is not the same for closed and open centres. These values of K, K^{cl} and K^{op}, can be obtained from fluorescence induction experiments with DCMU and dithionite treated leaves (see Vernotte *et al*., 1979). According to the Stern–Volmer equation:

$$\frac{F_M^{DCMU+dithionite}}{F_M^{DCMU}} = \frac{1}{1-f^{cl}} = 1 + K^{cl}[PQ]_{total}, \tag{A.2}$$

and

$$\frac{F_0^{DCMU+dithionite}}{F_0^{DCMU}} = \frac{1}{1-f^{op}} = 1 + K^{op}[PQ]_{total}. \tag{A.3}$$

where f^{cl} and f^{op} are the fractions of the fluorescence intensity that have been reduced by PQ non-photochemical quenching for a system with all PS II units closed and open, respectively. The values of f^{cl} and f^{op}, measured in chloroplasts by Vernotte *et al*. (1979), have been 20–30% and 5–10%, respectively.

For a heterogeneous PS II population (i.e. with open and closed units) the ratio between the unquenched and quenched fluorescence can be written as:

$$\frac{F^u(t)}{F(t)} = 1 + K\,(t)[PQ](t) \tag{A.4}$$

where $K(t)$ is a function depending on K^{cl} and K^{op}, which was approximated with the relationship:

$$K(t) = B(t)(K^{cl} - K^{op}) + K^{op}. \tag{A.5}$$

We have also assumed that the fraction of closed centres does not depend on this non-photochemical quenching by oxidised PQ.

The relative variable fluorescence $V(t) = [F(t) - F_0]/(F_M - F_0)$ can be written as a function of the experimental ratio $N = F_V/F_0 = (F_M - F_0)/F_0$, where F_V is the total variable fluorescence, F_0 the initial fluorescence, and F_M the maximum value of the fluorescence. We have:

$$V(t) = \frac{1}{N}\left(\frac{F(t)}{F_0} - 1\right). \tag{A.6}$$

A semi-empirical relationship of the relative variable fluorescence, $V(t)$, as a function of the unquenched relative variable fluorescence, $V^u(t)$, was obtained using eqs (A.4)–(A.6):

$$V(t) = \frac{K_0[PQ]_0 - K(t)[PQ](t)}{N(1 + K(t)[PQ](t))} + V^u(t)\frac{(N+1)(1 + K_M[PQ]_M) - (1 + K_0[PQ]_0)}{N(1 + K(t)[PQ](t))} \tag{A.7}$$

where: K_0 = the initial value of $K(t)$, K_M = the maximal value of $K(t)$, $[PQ]_0$ = the initial value of $[PQ](t)$, and $[PQ]_M$ = the value of $[PQ](t)$ corrspond-ing to K_M.

Glossary

$B(t)$:	fraction of the closed PS II centres at time t
B_{max}:	highest value of theoretical $B(t)$
C:	connectivity parameter, a numerical constant depending on the degree of connectivity between the PSII units [see the eqns (1) and (2)]
$F(t)$:	fluorescence at time t
F_M:	maximal fluorescence
F_M^{DCMU}:	maximal fluorescence in the presence of DCMU
$F_M^{DCMU+dithionite}$:	maximal fluorescence in the presence of DCMU and dithionite
F_0^{DCMU}:	initial fluorescence in the presence of DCMU
$F_0^{DCMU+dithionite}$:	*initial fluorescence in the presence of DCMU and dithionite*
F_0:	initial fluorescence
F_P:	fluorescence at the peak of the transient
F_V:	total variable fluorescence, equal to $F_M - F_0$
f^{cl} and f^{op}:	fraction of the fluorescence quenching for all closed and all open PS II centres respectively
K:	Stern–Volmer constant
$K(t)$:	theoretical Stern–Volmer "constant" for a system with both closed and open PS II centres at time t
K^{cl} and K^{op}:	Stern–Volmer constant for all closed and all open PS II centres respectively
K_M:	maximal value of $K(t)$
K_0:	initial value of $K(t)$
k^1_{AB} and k^1_{BA}:	forward and backward rate constants of the first reduction of Q_B by Q_A^-
k^2_{AB} and k^2_{BA}:	forward and backward rate constants of the second reduction of Q_B by Q_A^-
k_E and k_{-E}:	forward and backward rate constants of the exchange reaction between Q_BH_2 and PQ from the pool
k_H and k_{-H}:	forward and backward rate constants of Q_B^{2-} protonation
k^{ox}_{PQH2}:	rate constant of plastoquinol oxidation
kL:	global rate constant of the light reaction leading to Q_A reduction
kL^0:	initial rate constant of the light reaction leading to Q_A reduction
kL_0, kL_1, kL_2, and kL_3:	rate constants of the light reaction leading to Q_A reduction for PS II units with OEC in S_0, S_1, S_2 and S_3 states, respectively
kL^0_0, kL^0_1, kL^0_2, and kL^0_3:	initial rate constants of the light reaction leading to Q_A reduction for PS II units with OEC in S_0, S_1 , S_2 and S_3 states, respectively

kS_0, kS_1, kS_2 and kS_3: rate constants of the transitions from S_0 to S_1, S_1 to S_2, S_2 to S_3 and S_3 to S_0, respectively
$[PQ](t)$: plastoquinone pool concentration at time t
$[PQ]_0$: initial value of $[PQ](t)$
$[PQ]_M$: value of $[PQ](t)$ at the specific time when $K(t)$ has its maximal value (K_M)

$[PQ]_{total}$: total plastoquinone pool concentration
$[Q_A]_{total}$: concentration of PS II units with oxidised Q_A (open reaction centres)
$[Q_A^-]_{total}$: concentration of PS II units with reduced Q_A (closed reaction centres)

$Q_A^-Q_B$, $Q_A^-Q_B^-$, $Q_A^-Q_B^{2-}$, $Q_A^-Q_BH_2$,
$Q_AQ_B^-$, $Q_AQ_B^{2-}$, and $Q_AQ_BH_2$: PS II units with different redox states of Q_A and Q_B acceptors
N: ratio F_V/F_0
S_0, S_1, S_2, and S_3: redox states of OEC in PS II unit
$[S_nQ_AQ_B]_{total}$: total concentration of PS II units
$V(t)$: relative variable fluorescence at time t
V_{max}: highest value of theoretical $V(t)$
$V^u(t)$: relative variable fluorescence without plastoquinone quenching at time t
V^u_{max}: highest value of theoretical $V^u(t)$
$\varphi_P(t)$, φ_{Po}: quantum yield of the excitation energy trapping by an open PS II centre at time t,and at $t = 0$

Abbreviations

PS I and II: photosystem I and II
D1 and D2: major polypeptides of the reaction centre of PS II
Chl *a*: chlorophyll *a*
P680: primary electron donor of PS II
Phe: pheophytin *a*
Q_A, Q_B: primary and secondary quinone acceptor of PS II
PQ: plastoquinone
PQH_2: plastoquinol
Y_Z: primary electron donor to $P680^+$ (a tyrosine residue situated on D1)
Y_D: a tyrosine residue situated on D2
OEC: oxygen evolving complex
PC: plastocyanin
Cyt b/f: cytochrome b_6/f complex
P700: primary electron donor of PS I
S_n states: redox states of OEC
DCMU: 3-(3,4-dichlorphenyl)-1,1-dimethylurea
ODEs: Ordinary Differential Equations systems